Measurements of the Z Partial Decay Width into $c\bar{c}$ and Multiplicity of Charm Quarks per b Decay

DELPHI Collaboration

Abstract

The partial decay width R_c of the Z into $c\bar{c}$ quark pair and the number of charm quarks n_c per b decay are measured with the DELPHI detector at LEP 1. Particle identification provides clear D^0, D^+, D_s^+ and Λ_c^+ signatures. The charm hadron production rate is measured in each channel by a fit to the scaled energy, impact parameter information and the invariant mass spectrum. Two R_c measurements are presented, from the D^{*+} production rate and from the overall charm counting in $c\bar{c}$ events. The multiplicity n_c is inferred from the charm counting in $b\bar{b}$ events. The final results obtained for R_c and n_c are:

$$R_c = 0.1665 \pm 0.0095$$
$$n_c = 1.166 \pm 0.086\,.$$

P.Abreu[21], W.Adam[50], T.Adye[36], P.Adzic[11], I.Ajinenko[42], Z.Albrecht[17], T.Alderweireld[2], G.D.Alekseev[16], R.Alemany[49], T.Allmendinger[17], P.P.Allport[22], S.Almehed[24], U.Amaldi[9], S.Amato[47], E.G.Anassontzis[3], P.Andersson[44], A.Andreazza[9], S.Andringa[21], P.Antilogus[25], W-D.Apel[17], Y.Arnoud[9], B.Åsman[44], J-E.Augustin[25], A.Augustinus[9], P.Baillon[9], P.Bambade[19], F.Barao[21], G.Barbiellini[46], R.Barbier[25], D.Y.Bardin[16], G.Barker[9], A.Baroncelli[38], M.Battaglia[15], M.Baubillier[23], K-H.Becks[52], M.Begalli[6], P.Beilliere[8], Yu.Belokopytov[9,53], A.C.Benvenuti[5], C.Berat[14], M.Berggren[25], D.Bertini[25], D.Bertrand[2], M.Besancon[39], F.Bianchi[45], M.Bigi[45], M.S.Bilenky[16], M-A.Bizouard[19], D.Bloch[10], H.M.Blom[30], M.Bonesini[27], W.Bonivento[27], M.Boonekamp[39], P.S.L.Booth[22], A.W.Borgland[4], G.Borisov[19], C.Bosio[41], O.Botner[48], E.Boudinov[30], B.Bouquet[19], C.Bourdarios[19], T.J.V.Bowcock[22], I.Boyko[16], I.Bozovic[11], M.Bozzo[13], P.Branchini[38], T.Brenke[52], R.A.Brenner[48], P.Bruckman[18], J-M.Brunet[8], L.Bugge[32], T.Buran[32], T.Burgsmueller[52], P.Buschmann[52], S.Cabrera[49], M.Caccia[27], M.Calvi[27], T.Camporesi[9], V.Canale[37], F.Carena[9], L.Carroll[22], C.Caso[13], M.V.Castillo Gimenez[49], A.Cattai[9], F.R.Cavallo[5], V.Chabaud[9], Ph.Charpentier[9], L.Chaussard[25], P.Checchia[35], G.A.Chelkov[16], R.Chierici[45], P.Chliapnikov[42], P.Chochula[7], V.Chorowicz[25], J.Chudoba[29], K.Cieslik[18], P.Collins[9], R.Contri[13], E.Cortina[49], G.Cosme[19], F.Cossutti[9], J-H.Cowell[22], H.B.Crawley[1], D.Crennell[36], S.Crepe[14], G.Crosetti[13], J.Cuevas Maestro[33], S.Czellar[15], G.Damgaard[28], M.Davenport[9], W.Da Silva[23], A.Deghorain[2], G.Della Ricca[46], P.Delpierre[26], N.Demaria[9], A.De Angelis[9], W.De Boer[17], S.De Brabandere[2], C.De Clercq[2], B.De Lotto[46], A.De Min[35], L.De Paula[47], H.Dijkstra[9], L.Di Ciaccio[37], J.Dolbeau[8], K.Doroba[51], M.Dracos[10], J.Drees[52], M.Dris[31], A.Duperrin[25], J-D.Durand[9], G.Eigen[4], T.Ekelof[48], G.Ekspong[44], M.Ellert[48], M.Elsing[9], J-P.Engel[10], B.Erzen[43], M.Espirito Santo[21], E.Falk[24], G.Fanourakis[11], D.Fassouliotis[11], J.Fayot[23], M.Feindt[17], P.Ferrari[27], A.Ferrer[49], E.Ferrer-Ribas[19], S.Fichet[23], A.Firestone[1], U.Flagmeyer[52], H.Foeth[9], E.Fokitis[31], F.Fontanelli[13], B.Franek[36], A.G.Frodesen[4], R.Fruhwirth[50], F.Fulda-Quenzer[19], J.Fuster[49], A.Galloni[22], D.Gamba[45], S.Gamblin[19], M.Gandelman[47], C.Garcia[49], C.Gaspar[9], M.Gaspar[47], U.Gasparini[35], Ph.Gavillet[9], E.N.Gazis[31], D.Gele[10], L.Gerdyukov[42], N.Ghodbane[25], I.Gil[49], F.Glege[52], R.Gokieli[9,51], B.Golob[43], G.Gomez-Ceballos[40], P.Goncalves[21], I.Gonzalez Caballero[40], G.Gopal[36], L.Gorn[1,54], M.Gorski[51], Yu.Gouz[42], V.Gracco[13], J.Grahl[1], E.Graziani[38], C.Green[22], H-J.Grimm[17], P.Gris[39], G.Grosdidier[19], K.Grzelak[51], M.Gunther[48], J.Guy[36], F.Hahn[9], S.Hahn[52], S.Haider[9], A.Hallgren[48], K.Hamacher[52], J.Hansen[32], F.J.Harris[34], V.Hedberg[24], S.Heising[17], J.J.Hernandez[49], P.Herquet[2], H.Herr[9], T.L.Hessing[34], J.-M.Heuser[52], E.Higon[49], S-O.Holmgren[44], P.J.Holt[34], S.Hoorelbeke[2], M.Houlden[22], J.Hrubec[50], K.Huet[2], G.J.Hughes[22], K.Hultqvist[44], J.N.Jackson[22], R.Jacobsson[9], P.Jalocha[9], R.Janik[7], Ch.Jarlskog[24], G.Jarlskog[24], P.Jarry[39], B.Jean-Marie[19], E.K.Johansson[44], P.Jonsson[25], C.Joram[9], P.Juillot[10], F.Kapusta[23], K.Karafasoulis[11], S.Katsanevas[25], E.C.Katsoufis[31], R.Keranen[17], B.P.Kersevan[43], B.A.Khomenko[16], N.N.Khovanski[16], A.Kiiskinen[15], B.King[22], A.Kinvig[22], N.J.Kjaer[30], O.Klapp[52], H.Klein[9], P.Kluit[30], P.Kokkinias[11], M.Koratzinos[9], V.Kostioukhine[42], C.Kourkoumelis[3], O.Kouznetsov[39], E.Kriznic[43], P.Krstic[11], Z.Krumstein[16], P.Kubinec[7], J.Kurowska[51], K.Kurvinen[15], J.W.Lamsa[1], D.W.Lane[1], P.Langefeld[52], V.Lapin[42], J-P.Laugier[39], R.Lauhakangas[15], G.Leder[50], F.Ledroit[14], V.Lefebure[2], L.Leinonen[44], A.Leisos[11], R.Leitner[29], J.Lemonne[2], G.Lenzen[52], V.Lepeltier[19], T.Lesiak[18], M.Lethuillier[39], J.Libby[34], D.Liko[9], A.Lipniacka[44], I.Lippi[35], B.Loerstad[24], J.G.Loken[34], J.H.Lopes[47], J.M.Lopez[40], R.Lopez-Fernandez[14], D.Loukas[11], P.Lutz[39], L.Lyons[34], J.MacNaughton[50], J.R.Mahon[6], A.Maio[21], A.Malek[52], T.G.M.Malmgren[44], V.Malychev[16], F.Mandl[50], J.Marco[40], R.Marco[40], B.Marechal[47], M.Margoni[35], J-C.Marin[9], C.Mariotti[9], A.Markou[11], C.Martinez-Rivero[19], F.Martinez-Vidal[49], S.Marti i Garcia[9], J.Masik[12], N.Mastroyiannopoulos[11], F.Matorras[40], C.Matteuzzi[27], G.Matthiae[37], F.Mazzucato[35], M.Mazzucato[35], M.Mc Cubbin[22], R.Mc Kay[1], R.Mc Nulty[22], G.Mc Pherson[22], C.Meroni[27], W.T.Meyer[1], A.Miagkov[42], E.Migliore[45], L.Mirabito[25], W.A.Mitaroff[50], U.Mjoernmark[24], T.Moa[44], M.Moch[17], R.Moeller[28], K.Moenig[9], M.R.Monge[13], X.Moreau[23], P.Morettini[13], G.Morton[34], U.Mueller[52], K.Muenich[52], M.Mulders[30], C.Mulet-Marquis[14], R.Muresan[24], W.J.Murray[36], B.Muryn[14,18], G.Myatt[34], T.Myklebust[32], F.Naraghi[14], F.L.Navarria[5], S.Navas[49], K.Nawrocki[51], P.Negri[27], S.Nemecek[12], N.Neufeld[9], N.Neumeister[50], R.Nicolaidou[39], B.S.Nielsen[28], M.Nikolenko[10,16], V.Nomokonov[15], A.Normand[22], A.Nygren[24], V.Obraztsov[42], A.G.Olshevski[16], A.Onofre[21], R.Orava[15], G.Orazi[10], K.Osterberg[15], A.Ouraou[39], M.Paganoni[27], S.Paiano[5], R.Pain[23], R.Paiva[21], J.Palacios[34], H.Palka[18], Th.D.Papadopoulou[31], K.Papageorgiou[11], L.Pape[9], C.Parkes[9], F.Parodi[13], U.Parzefall[22], A.Passeri[38], O.Passon[52], M.Pegoraro[35], L.Peralta[21], M.Pernicka[50], A.Perrotta[5], C.Petridou[46], A.Petrolini[13], H.T.Phillips[36], F.Pierre[39], M.Pimenta[21], E.Piotto[27], T.Podobnik[43], M.E.Pol[6], G.Polok[18], P.Poropat[46], V.Pozdniakov[16], P.Privitera[37], N.Pukhaeva[16], A.Pullia[27], D.Radojicic[34], S.Ragazzi[27], H.Rahmani[31], D.Rakoczy[50], P.N.Ratoff[20], A.L.Read[32], P.Rebecchi[9], N.G.Redaelli[27], M.Regler[50], D.Reid[30], R.Reinhardt[52], P.B.Renton[34], L.K.Resvanis[3], F.Richard[19], J.Ridky[12], G.Rinaudo[45], O.Rohne[32], A.Romero[45], P.Ronchese[35], E.I.Rosenberg[1], P.Rosinsky[7], P.Roudeau[19], T.Rovelli[5], Ch.Royon[39], V.Ruhlmann-Kleider[39], A.Ruiz[40], H.Saarikko[15], Y.Sacquin[39], A.Sadovsky[16], G.Sajot[14], J.Salt[49], D.Sampsonidis[11], M.Sannino[13], H.Schneider[17], Ph.Schwemling[23], U.Schwickerath[17], M.A.E.Schyns[52], F.Scuri[46], P.Seager[20], Y.Sedykh[16], A.M.Segar[34], R.Sekulin[36], R.C.Shellard[6], A.Sheridan[22], M.Siebel[52], L.Simard[39], F.Simonetto[35], A.N.Sisakian[16], G.Smadja[25], O.Smirnova[24], G.R.Smith[36], A.Sokolov[42], A.Sopczak[17],

R.Sosnowski[51], T.Spassov[21], E.Spiriti[38], P.Sponholz[52], S.Squarcia[13], D.Stampfer[50], C.Stanescu[38], S.Stanic[43], K.Stevenson[34], A.Stocchi[19], J.Strauss[50], R.Strub[10], B.Stugu[4], M.Szczekowski[51], M.Szeptycka[51], T.Tabarelli[27], O.Tchikilev[42], F.Tegenfeldt[48], F.Terranova[27], J.Thomas[34], J.Timmermans[30], N.Tinti[5], L.G.Tkatchev[16], S.Todorova[10], A.Tomaradze[2], B.Tome[21], A.Tonazzo[9], L.Tortora[38], G.Transtromer[24], D.Treille[9], G.Tristram[8], M.Trochimczuk[51], C.Troncon[27], A.Tsirou[9], M-L.Turluer[39], I.A.Tyapkin[16], S.Tzamarias[11], B.Ueberschaer[52], O.Ullaland[9], V.Uvarov[42], G.Valenti[5], E.Vallazza[46], C.Vander Velde[2], G.W.Van Apeldoorn[30], P.Van Dam[30], W.K.Van Doninck[2], J.Van Eldik[30], A.Van Lysebetten[2], I.Van Vulpen[30], N.Vassilopoulos[34], G.Vegni[27], L.Ventura[35], W.Venus[36,9], F.Verbeure[2], M.Verlato[35], L.S.Vertogradov[16], V.Verzi[37], D.Vilanova[39], L.Vitale[46], E.Vlasov[42], A.S.Vodopyanov[16], C.Vollmer[17], G.Voulgaris[3], V.Vrba[12], H.Wahlen[52], C.Walck[44], C.Weiser[17], D.Wicke[52], J.H.Wickens[2], G.R.Wilkinson[9], M.Winter[10], M.Witek[18], G.Wolf[9], J.Yi[1], O.Yushchenko[42], A.Zalewska[18], P.Zalewski[51], D.Zavrtanik[43], E.Zevgolatakos[11], N.I.Zimin[16,24], G.C.Zucchelli[44], G.Zumerle[35]

[1]Department of Physics and Astronomy, Iowa State University, Ames IA 50011-3160, USA
[2]Physics Department, Univ. Instelling Antwerpen, Universiteitsplein 1, BE-2610 Wilrijk, Belgium
 and IIHE, ULB-VUB, Pleinlaan 2, BE-1050 Brussels, Belgium
 and Faculté des Sciences, Univ. de l'Etat Mons, Av. Maistriau 19, BE-7000 Mons, Belgium
[3]Physics Laboratory, University of Athens, Solonos Str. 104, GR-10680 Athens, Greece
[4]Department of Physics, University of Bergen, Allégaten 55, NO-5007 Bergen, Norway
[5]Dipartimento di Fisica, Università di Bologna and INFN, Via Irnerio 46, IT-40126 Bologna, Italy
[6]Centro Brasileiro de Pesquisas Físicas, rua Xavier Sigaud 150, BR-22290 Rio de Janeiro, Brazil
 and Depto. de Física, Pont. Univ. Católica, C.P. 38071 BR-22453 Rio de Janeiro, Brazil
 and Inst. de Física, Univ. Estadual do Rio de Janeiro, rua São Francisco Xavier 524, Rio de Janeiro, Brazil
[7]Comenius University, Faculty of Mathematics and Physics, Mlynska Dolina, SK-84215 Bratislava, Slovakia
[8]Collège de France, Lab. de Physique Corpusculaire, IN2P3-CNRS, FR-75231 Paris Cedex 05, France
[9]CERN, CH-1211 Geneva 23, Switzerland
[10]Institut de Recherches Subatomiques, IN2P3 - CNRS/ULP - BP20, FR-67037 Strasbourg Cedex, France
[11]Institute of Nuclear Physics, N.C.S.R. Demokritos, P.O. Box 60228, GR-15310 Athens, Greece
[12]FZU, Inst. of Phys. of the C.A.S. High Energy Physics Division, Na Slovance 2, CZ-180 40, Praha 8, Czech Republic
[13]Dipartimento di Fisica, Università di Genova and INFN, Via Dodecaneso 33, IT-16146 Genova, Italy
[14]Institut des Sciences Nucléaires, IN2P3-CNRS, Université de Grenoble 1, FR-38026 Grenoble Cedex, France
[15]Helsinki Institute of Physics, HIP, P.O. Box 9, FI-00014 Helsinki, Finland
[16]Joint Institute for Nuclear Research, Dubna, Head Post Office, P.O. Box 79, RU-101 000 Moscow, Russian Federation
[17]Institut für Experimentelle Kernphysik, Universität Karlsruhe, Postfach 6980, DE-76128 Karlsruhe, Germany
[18]Institute of Nuclear Physics and University of Mining and Metalurgy, Ul. Kawiory 26a, PL-30055 Krakow, Poland
[19]Université de Paris-Sud, Lab. de l'Accélérateur Linéaire, IN2P3-CNRS, Bât. 200, FR-91405 Orsay Cedex, France
[20]School of Physics and Chemistry, University of Lancaster, Lancaster LA1 4YB, UK
[21]LIP, IST, FCUL - Av. Elias Garcia, 14-1º, PT-1000 Lisboa Codex, Portugal
[22]Department of Physics, University of Liverpool, P.O. Box 147, Liverpool L69 3BX, UK
[23]LPNHE, IN2P3-CNRS, Univ. Paris VI et VII, Tour 33 (RdC), 4 place Jussieu, FR-75252 Paris Cedex 05, France
[24]Department of Physics, University of Lund, Sölvegatan 14, SE-223 63 Lund, Sweden
[25]Université Claude Bernard de Lyon, IPNL, IN2P3-CNRS, FR-69622 Villeurbanne Cedex, France
[26]Univ. d'Aix - Marseille II - CPP, IN2P3-CNRS, FR-13288 Marseille Cedex 09, France
[27]Dipartimento di Fisica, Università di Milano and INFN, Via Celoria 16, IT-20133 Milan, Italy
[28]Niels Bohr Institute, Blegdamsvej 17, DK-2100 Copenhagen Ø, Denmark
[29]NC, Nuclear Centre of MFF, Charles University, Areal MFF, V Holesovickach 2, CZ-180 00, Praha 8, Czech Republic
[30]NIKHEF, Postbus 41882, NL-1009 DB Amsterdam, The Netherlands
[31]National Technical University, Physics Department, Zografou Campus, GR-15773 Athens, Greece
[32]Physics Department, University of Oslo, Blindern, NO-1000 Oslo 3, Norway
[33]Dpto. Fisica, Univ. Oviedo, Avda. Calvo Sotelo s/n, ES-33007 Oviedo, Spain
[34]Department of Physics, University of Oxford, Keble Road, Oxford OX1 3RH, UK
[35]Dipartimento di Fisica, Università di Padova and INFN, Via Marzolo 8, IT-35131 Padua, Italy
[36]Rutherford Appleton Laboratory, Chilton, Didcot OX11 OQX, UK
[37]Dipartimento di Fisica, Università di Roma II and INFN, Tor Vergata, IT-00173 Rome, Italy
[38]Dipartimento di Fisica, Università di Roma III and INFN, Via della Vasca Navale 84, IT-00146 Rome, Italy
[39]DAPNIA/Service de Physique des Particules, CEA-Saclay, FR-91191 Gif-sur-Yvette Cedex, France
[40]Instituto de Fisica de Cantabria (CSIC-UC), Avda. los Castros s/n, ES-39006 Santander, Spain
[41]Dipartimento di Fisica, Università degli Studi di Roma La Sapienza, Piazzale Aldo Moro 2, IT-00185 Rome, Italy
[42]Inst. for High Energy Physics, Serpukov P.O. Box 35, Protvino, (Moscow Region), Russian Federation
[43]J. Stefan Institute, Jamova 39, SI-1000 Ljubljana, Slovenia and Laboratory for Astroparticle Physics,
 Nova Gorica Polytechnic, Kostanjeviska 16a, SI-5000 Nova Gorica, Slovenia,
 and Department of Physics, University of Ljubljana, SI-1000 Ljubljana, Slovenia
[44]Fysikum, Stockholm University, Box 6730, SE-113 85 Stockholm, Sweden
[45]Dipartimento di Fisica Sperimentale, Università di Torino and INFN, Via P. Giuria 1, IT-10125 Turin, Italy
[46]Dipartimento di Fisica, Università di Trieste and INFN, Via A. Valerio 2, IT-34127 Trieste, Italy
 and Istituto di Fisica, Università di Udine, IT-33100 Udine, Italy
[47]Univ. Federal do Rio de Janeiro, C.P. 68528 Cidade Univ., Ilha do Fundão BR-21945-970 Rio de Janeiro, Brazil
[48]Department of Radiation Sciences, University of Uppsala, P.O. Box 535, SE-751 21 Uppsala, Sweden
[49]IFIC, Valencia-CSIC, and D.F.A.M.N., U. de Valencia, Avda. Dr. Moliner 50, ES-46100 Burjassot (Valencia), Spain
[50]Institut für Hochenergiephysik, Österr. Akad. d. Wissensch., Nikolsdorfergasse 18, AT-1050 Vienna, Austria
[51]Inst. Nuclear Studies and University of Warsaw, Ul. Hoza 69, PL-00681 Warsaw, Poland
[52]Fachbereich Physik, University of Wuppertal, Postfach 100 127, DE-42097 Wuppertal, Germany
[53]On leave of absence from IHEP Serpukhov
[54]Now at University of Florida

1 Introduction

A precise determination of the partial decay width $R_c = \frac{\Gamma_c}{\Gamma_{had}}$ of the Z into $c\bar{c}$ quark pairs provides a fundamental test of the Standard Model. The measurement of the number of charm quarks n_c per b decay is an important input to resolve the discrepancy between the experimental value of $BR(b \to l\nu X)$ and its theoretical prediction [1]. This paper presents a simultaneous measurement of these quantities using the charm counting technique [2,24] and an R_c measurement using D^{*+} mesons [4].

The measured rate of D or Λ_c hadrons is given by $2R_{c(b)}P_{c(b) \to D,\Lambda_c}$, multiplying the partial decay width $R_{c(b)} = \frac{\Gamma_{c(b)}}{\Gamma_{had}}$ and the probability $P_{c(b) \to D,\Lambda_c}$ of the quark to produce a given charm hadron. A c quark always gives a charm hadron, but a b hadron can decay into a D or c baryon as well as into a pair of charm hadrons [1]. For $c\bar{c}$ events, the sum over the probabilities $P_{c \to D,\Lambda_c}$ for all weakly decaying charm hadrons adds up to one. Hence R_c can be extracted from the sum of the rates. Furthermore the probability $P_{c \to D^{*+}}$ has been measured in DELPHI [5], using low energy pions from D^{*+} decays tagged by exclusively reconstructed D mesons in the opposite hemisphere. Thus the measurement of the D^{*+} rate in $c\bar{c}$ events, $R_c P_{c \to D^{*+}}$, also allows an independent measurement of R_c. In $b\bar{b}$ events the sum of the production probabilities is a direct measurement of the number of charm quarks n_c per b decay. The large number of events collected at LEP 1 leads to significant improvements in the precision. This analysis uses the data taken by DELPHI between 1992 and 1995.

Separation between $c\bar{c}$ and $b\bar{b}$ events is necessary. A fit of the simulated b and c contributions to the measured impact parameter information, scaled charm hadron energy $X_E = 2E_D/\sqrt{s}$ and invariant mass spectrum is used to separate the classes.

In this analysis charm hadrons are reconstructed in the following decay modes [2]:

$D^0 \to K^-\pi^+$,
$D^+ \to K^-\pi^+\pi^+$,
$D_s^+ \to \phi(1020)\pi^+$ and $D_s^+ \to \bar{K}^*(892)K^+$,
$\Lambda_c^+ \to pK^-\pi^+$,
$D^{*+} \to D^0\pi^+$ with $D^0 \to K^-\pi^+$.

The combinatorial background is much reduced by identifying kaons and protons in the charm hadron decay products using particle identification information provided by the DELPHI Ring Imaging Cherenkov Counters (RICH) and the measured energy loss by ionisation in the Time Projection Chamber (TPC).

2 The DELPHI detector

The DELPHI detector consists of several independent devices for tracking, calorimetry, lepton and particle identification. Only the tracking and particle identification components are relevant for this analysis and will be briefly described in the following. A detailed description of the whole apparatus and its performance can be found in [7].

Looking from the interaction point through the detector, the closest tracking device is the Vertex Detector (VD). The LEP 1 version of the VD had three concentric layers of silicon microstrip modules with the outer layer having 11 cm radius. Since 1994 the single sided closer and outer layers have been replaced by double sided modules. With an intrinsic $R\phi$ resolution, transverse to the beam axis, of 7.6 μm [7], the VD is the

---

[1]There is no distinction between c-hadron and anti-c hadron in the present definition of $P_{c(b) \to D,\Lambda_c}$.

[2]Throughout this paper charge-conjugate states are implicitly included.

main component to reconstruct secondary vertices of heavy hadron decays. The VD is followed by the Inner Detector (ID) which consists of a jet chamber part and trigger layers. The Time Projection Chamber (TPC) is the main tracking device in DELPHI. Charged particles are measured with a precision of approximately 250 μm in $R\phi$ and 880 μm along the beam axis [7]. The 192 sense wires measure the energy loss of charged particles, dE/dx. The outermost tracking component for the barrel region is the Outer Detector (OD), made of 5 layers of drift tubes.

The DELPHI Barrel RICH is placed between the TPC and the Outer Detector. Two radiators enable it to identify pions, kaons and protons over nearly the full momentum range.

The tracking of charged particles is extended to the forward region by two wire chambers FCA and FCB. FCA is mounted on the endcap of the TPC and covers a polar angle range from 11° to 32° and 148° to 169°, while FCB is placed behind the forward RICH on both sides of the DELPHI endcaps. FCB covers the polar angle range from 11° to 36° and 144° to 169°.

3 Event selection and simulation

Charged particles were selected as follows. The momentum was required to be between 0.4 GeV/c and 50 GeV/c, the relative error on the momentum measurement less than 1, the polar angle relative to the beam axis between 20° and 160°, the length of tracks with TPC hits over 30 cm, the projection of the impact parameter relative to the interaction point had to be less than 4 cm in the plane transverse to the beam direction and the distance to the interaction point along the beam direction less than 10 cm.

Hadronic events were selected by requiring five or more charged particles and a total energy of charged particles larger than 12% of the centre-of-mass energy, assuming all charged particles to be pions. A total of 3.5 million hadronic events was obtained from the 1992-1995 data, at centre-of-mass energies within 2 GeV of the Z resonance mass. According to the simulation, the selection efficiency for hadronic Z decays was 95.7%. The sample also contained 0.24% of τ pair and 0.19% of Bhabha events. The bias due to this contamination is taken into account in the analysis. All other background sources were found to be negligible.

For each event, the primary interaction vertex was determined from the measured tracks with a constraint on the measured mean beam spot position. The fit was iterated by removing the track giving the biggest contribution to χ^2 until either the χ^2/NDF of all contributing tracks was less than 3 or only two tracks were left. All track parameters were then redefined after a helix extrapolation to this vertex position. The resolution of charged particles measured only by the forward tracking chambers was improved by a track refit using the primary vertex. Such forward tracks having a fit χ^2 larger than 100 are mostly due to secondary interactions and were removed from the analysis.

The simulation was done with the JETSET 7.3 Parton Shower model [8] using DELPHI tuned parameters obtained from a fit to event shape distributions and identified particle spectra [9]. The heavy hadron decay tables were modified. D^{**} and B^{**} production was included with fractions of 30% B^{**} in $b\bar{b}$ events and 30% D^{**} in $c\bar{c}$ events. The fragmentation function used for b and c quarks was that of Peterson et al. [10]:

$$f(z) \propto \left[z \left(1 - \frac{1}{z} - \frac{\epsilon_q}{1-z} \right)^2 \right]^{-1} \tag{1}$$

where z is the fraction $(E + p_{\parallel})_{hadron}/(E + p_{\parallel})_{quark}$ with $p_{\parallel}$ the momentum component parallel to the quark direction. The $\epsilon_{q=b,c}$ parameters were adjusted to central values of $\epsilon_b = 0.00233$ and $\epsilon_c = 0.0305$ in order to reproduce the average energy fractions $\langle X_E^b(B) \rangle = 0.702 \pm 0.008$ and $\langle X_E^c(D^*) \rangle = 0.510 \pm 0.005 \pm 0.008$ taken by B and D^* hadrons in Z events [11], respectively.

4 Charm hadron reconstruction

Candidates for the charm hadron decays $D^0 \rightarrow K^- \pi^+$, $D^+ \rightarrow K^- \pi^+ \pi^+$, $D_s^+ \rightarrow \phi(1020)\pi^+$, $D_s^+ \rightarrow \bar{K}^*(892)K^+$ and $\Lambda_c^+ \rightarrow pK^- \pi^+$ were reconstructed from all possible combinations of charged particles with a momentum larger than 1 (2) GeV/c for pion and kaon (proton) candidates. For $D^{*+} \rightarrow D^0 \pi^+$ followed by $D^0 \rightarrow K^- \pi^+$ candidates, the small mass difference between the D^{*+} and the decaying D^0 allowed the definition of a signal with a good signal-to-noise ratio. For this channel, the pion from the D^{*+} decay was selected with the default momentum (larger than 0.4 GeV/c). For D_s^+ candidates, a minimum momentum of 3 GeV/c was required for the ϕ and $\bar{K}^*$ and the invariant masses of ϕ and $\bar{K}^*$ had to be within $1.01 - 1.03$ GeV/c^2 and $0.86 - 0.94$ GeV/c^2, respectively.

In order to remove badly measured tracks from secondary interactions, all particles associated to the charm hadron candidate (except the D^{*+}) were required to have at least one associated VD hit. The charged particles of each decay channel were then used to fit a secondary vertex in space and the track parameters were recomputed at this common secondary vertex. The combinations of the charged particles for a given decay were retained if their invariant mass and scaled energy, X_E, satisfied the cuts given in table 1, where the X_E^{min} cuts were choosen to obtain a clear signature over a sufficiently low backgound.

Particle	mass (GeV/c^2)			X_E^{min}
D^0	1.80	-	2.20	0.30
D^+	1.70	-	2.05	0.20
D_s^+	1.90	-	2.20	0.20
Λ_c^+	2.10	-	2.50	0.30
D^0 from D^{*+}	1.79	-	1.94	0.15

Table 1: *Invariant mass range and minimum scaled energy for each channel.*

A cut on the helicity angle was applied to reject the combinatorial background. This quantity, Θ_h, was defined as the angle between the sphericity axis [13] of the decay products in the rest frame of the charm hadron (D or Λ) with respect to its direction of flight. The direction of the sphericity axis was given by the kaon (proton) as the leading particle in the computation. This angle is isotropic for pseudo-scalar decays while the combinatorial background has a clear enhancement at $\cos\Theta_h = \pm 1$. Since the background is concentrated at energies lower than those of charm hadrons, helicity angle dependent cuts on the energy were used:

$$X_E > a \cdot e^{+b(\cos\Theta_h - 1)} + c \quad \text{and} \quad X_E > a \cdot e^{-b(\cos\Theta_h + 1)} + c . \tag{2}$$

The a, b, c coefficients are listed in table 2.

The charm candidate's decay length, L, was calculated as the distance between the primary and the decay vertices in the plane transverse to the beam axis, projected on

Particle	a	b	c
D^0	0.5	2.0	0.20
D^+	0.5	3.0	0.10
D_s^+	0.5	2.2	0.10
Λ_c^+	0.5	3.0	0.15
D^0 from D^{*+}	0.5	3.0	0.10

Table 2: *Energy dependent cut values on the helicity angle.*

the charm direction of flight. The sign of the decay length was set negative if the decay vertex was behind the primary vertex with respect to the direction of flight. A positive value of L was required (except for the case of the D^{*+} decays) in order to remove the combinatorial background due to other particles from the primary vertex. The additional energy dependent decay length cut

$$L(X_E) > x \cdot (X_E - X_E^{min})^2 + y \tag{3}$$

gave a much lower combinatorial background level at high energies. The coefficients x and y are listed in table 3 for the different decay channels. The value X_E^{min} is given in table 1. No energy dependent cuts were used for the Λ_c and the $D_s^+(\bar{K}^*)$ samples.

Particle	x	y	L_{min} (cm)
D^0	-0.5	0.125	0.050
D^+	-1.0	0.230	0.125
$D_s^+(\phi)$	-1.0	0.100	0
$D_s^+(K^*)$	-	-	0.100
Λ_c^+	-	-	0.015

Table 3: *Minimum decay length and parameters for the energy-dependent decay length cut.*

For the $D_s^+(\phi)$ sample an additional selection was applied on the angle $\Theta_{K\pi}$ between one of the kaons from the ϕ and the remaining pion in the rest frame of the ϕ. This angle follows a $\cos^2(\Theta_{K\pi})$ distribution due to the decay of a pseudoscalar particle into a vector and a pseudoscalar particle, while the background is flat. A cut on $\cos(\Theta_{K\pi}) > 0.3$ was used for the $D_s^+(\phi)$ sample, whereas for the $D_s^+(\bar{K}^*)$ sample such a cut just lowered the overall reconstruction efficiency with no improvements in the signal to background ratio.

Another kinematical quantity used to remove the background was the χ^2 probability, $\mathcal{P}(\chi^2)$, of the secondary vertex fit performed with the tracks of the charm hadron decay products. For well measured secondary vertices the probability is flat between 0 and 1, while it peaks at 0 for wrong combinations. For the D^+ and Λ_c^+ decay modes, a cut of $\mathcal{P}(\chi^2) > 0.001$ was used, while a tighter cut of 0.01 was applied for both D_s^+ decay channels. No cut was applied on the decay vertex of the D^0 and the D^{*+}.

The particle identification provided by the RICH and the energy loss dE/dx measurement in the TPC were used to identify kaons and protons. The tagging of those particles coming from the charm hadron decays was done using standard DELPHI tagging routines for the RICH [14], based on the the measured Cherenkov angle information. The dE/dx

information [7] was only used if no RICH information was available. The tagging was done using the pull Δ_i :

$$\Delta_i = \frac{dE/dx(meas.) - dE/dx(exp.)}{\sigma(meas.)} \tag{4}$$

of the measured dE/dx with respect to the expected value for the kaon, pion or proton mass hypothesis i, provided by the Bethe-Bloch [15] formula. To separate kaons from pions or protons, a cut parameter tag_{TPC} was calculated on the basis of a simple ansatz for the probability density P_i^{TPC}:

$$tag_{TPC} = \frac{P_K^{TPC}}{P_K^{TPC} + P_\pi^{TPC}} \quad or \quad tag_{TPC} = \frac{P_p^{TPC}}{P_p^{TPC} + P_K^{TPC}} \tag{5}$$

$$P_i^{TPC} = e^{-\frac{1}{2}\Delta_i^2} \tag{6}$$

To ensure a good dE/dx measurement, quality flags similar to those used for the RICH information were tested which account for the number of participating wires and the track length in the TPC. For decay modes of the D^+, D_s^+ and Λ_c^+, a candidate kaon or proton was rejected if no RICH or dE/dx identification was available. No kaon identification was required for D^{*+} candidates because the D^0 mass selection already removes most of the background.

The D^0, D^+, D_s^+, Λ_c^+ and D^{*+} mass spectra obtained after these selections are shown in figures 1 and 2. Because of the small amount of RICH information available in 1992, these data were not used for the $D_s^+(\bar{K}^*)$ and Λ_c^+ samples. The reflections from other D decay modes are shown as the dotted lines. The dash-dotted line in the D^0 spectrum of figure 1 shows $K\pi$ combinations which were wrongly reconstructed as πK. D^+ decays into $K^- K^+ \pi^+$ or $K^- \pi^+ \pi^+$, where the wrong mass is assigned to one of the pions, are an important background in the D_s^+ spectrum, as can be seen from the dashed line in the D_s^+ spectra in figure 1. An additional cut was applied to the D^+ sample in order to remove the background from $D^{*+} \to D^0 \pi^+$ with $D^0 \to K^- \pi^+$ decays. The difference between the $K^- \pi^+ \pi^+$ and any of the $K^- \pi^+$ combinations had to be larger than 150 MeV/c^2. Table 4 shows the number of candidates obtained for each decay channel, after background subtraction.

Decay	$N_{candidates}$
$D^0 \to K^- \pi^+$	9076 ± 237
$D^+ \to K^- \pi^+ \pi^+$	7018 ± 200
$D_s^+ \to \phi \pi^+$	742 ± 64
$D_s^+ \to K^* K^+$	515 ± 61
$\Lambda_c^+ \to p K^- \pi^+$	336 ± 42
$D^{*+} \to (K^- \pi^+) \pi^+$	7872 ± 225

Table 4: *Number of candidates for the measured charm hadrons.*

5   Fit method

For a measurement of R_c and n_c, it is necessary to distinguish the charm production in $c\bar{c}$ and $b\bar{b}$ events to minimise the correlations. To achieve the best separation, the

scaled energy of the charm hadron was used together with the b tag impact parameter information [16] in a combined fit.

For each event the impact parameter information of each charged particle was used to define the probability $\mathcal{P}_{ev}$ that all tracks N were compatible with the primary vertex:

$$\mathcal{P}_{ev} \equiv \Pi \cdot \sum_{j=0}^{N-1} \frac{(-\ln\Pi)^j}{j!} \quad , \text{ with } \Pi \equiv \prod_{i=1}^{N} P(S_i) . \tag{7}$$

Here the $P(S_i)$ are probability functions which were computed from the resolution of the significance distribution [16]. In order to smooth the $\mathcal{P}_{ev}$ distribution, which peaks around zero for $b\bar{b}$ events, a transformation

$$tr(\mathcal{P}_{ev}) = \frac{4}{4 - \ln(\mathcal{P}_{ev})} \tag{8}$$

was applied. The selection of charm hadrons also resulted in a sample of events with tracks with large impact parameters. In particular for the D^+ the separation power from $\mathcal{P}_{ev}$ was lowered because of its long lifetime, which is close to the B mesons lifetime. Hence $\mathcal{P}_{ev}$ was computed only from particles in the event which were not associated to the charm hadron candidate. This decreased the correlation between the c and b results by 5% on average.

Combining $\mathcal{P}_{ev}$ with the scaled energy X_E of the charm hadron allowed the background from light quark events to be separated from $b\bar{b}$ and $c\bar{c}$ events. Charm hadrons from $c\bar{c}$ events have a harder X_E spectrum than those coming from B decays. Light quark events are expected to have large $tr(\mathcal{P}_{ev})$ and small X_E. $c\bar{c}$ events are concentrated at large $tr(\mathcal{P}_{ev})$ and large X_E, whereas $b\bar{b}$ events are at small X_E and small $tr(\mathcal{P}_{ev})$.

Particle	mass	X_E	$tr(\mathcal{P}_{ev})$	$\langle N_{i,j,k}^{dat} \rangle$
D^0	10	5	5	244
D^+	10	6	6	218
$D_s^+(\phi)$	10	5	5	21
$D_s^+(K^*)$	8	5	5	19
Λ_c^+	10	5	5	28
D^{*+}	10	5	5	146

Table 5: *Number of bins used in each dimension and the average number of events per bin.*

The fit of the charm hadron rates $R_q \cdot P_{q \to X} \cdot BR$ in $c\bar{c}$ and $b\bar{b}$ events used bins in three dimensions of invariant mass, X_E and $tr(\mathcal{P}_{ev})$. The number of bins in each dimension and the average number of data events per bin are listed in table 5. The width of each bin was chosen to keep the number of events per bin about constant. The fit was done with two different approaches, depending on the average number of entries per bin. For the D^0 and D^+ this number was around 230, for the D^{*+} around 150. A χ^2 fit was performed with:

$$\chi^2 = \sum_i^{mass} \sum_j^{tr(\mathcal{P}_{ev})} \sum_k^{X_E} \left(\frac{N_{i,j,k}^{dat} - \lambda_{i,j,k}}{\sigma_{i,j,k}} \right)^2 . \tag{9}$$

Here $N_{i,j,k}^{dat}$ is the number of candidates in a given bin, $\sigma_{i,j,k}$ is the quadratic sum of the statistical error of the data and the Monte Carlo prediction. The expected number of

candidates $\lambda_{i,j,k}$ was calculated assuming the Monte Carlo shape for the different classes. It is given by:

$$\lambda_{i,j,k} = \frac{2N_{had}}{\epsilon_{had}} \sum_{q=b,c,g \to c\bar{c}} R_q \cdot P_{q \to X} \cdot BR \cdot \frac{N_{i,j,k}^{acc}(q)}{N_{tot}^{gen}(q)} \tag{10}$$
$$+ N_{i,j,k}^{back} \cdot \eta_{j,k}^{back} + N_{i,j,k}^{reflect} .$$

The first term of this equation reflects the charm hadron signal with its contributions from $b\bar{b}$, $c\bar{c}$ and light quark events. The ratio of the number of reconstructed signal events $N_{i,j,k}^{acc}(q)$ to the generated ones $N_{tot}^{gen}(q)$ represents the flavour dependent shape of the simulated signal. N_{had} is the total number of hadronic events in the data and ϵ_{had} their selection efficiency.

The second term describes the Monte Carlo background shape. Here the $N_{i,j,k}^{back}$ values are the number of background events. The $\eta_{j,k}^{back}$ are additional background normalisations for each bin in X_E and $tr(\mathcal{P}_{ev})$. They are introduced to compensate for any effect in the Monte Carlo background description, which could slightly differ from the real data.

The fraction of charm hadrons from $b\bar{b}$ and $c\bar{c}$ events, $R_q P_{q \to X} BR$, as well as the background normalisation $\eta_{j,k}^{back}$ in each bin in X_E and $tr(\mathcal{P}_{ev})$ were free parameters in the fit. The rate of charm hadrons in light quark events was taken from the multiplicity of gluon splitting into heavy quarks [11].

The background normalisations for the D^0 and D^+, as determined in the fit with 5×5 and 6×6 bins in X_E and $tr(\mathcal{P}_{ev})$, had mean values of 0.978 ± 0.096 and 0.969 ± 0.097, where the errors are the statistical uncertainty.

The last contribution to the $\lambda_{i,j,k}$ is a term accounting for reflections from other decay modes which are particularly important in the channel $D_s^+(\bar{K}^*)$. Since it also depends on the $R_q P_{q \to X}$, it was treated as a separate class in the final fit with its shape taken directly from the simulation.

For the D_s^+ and Λ_c the average number of entries was only around 25. Therefore the number of entries per bin was no longer Gaussian distributed and Poissonian statistics was taken instead. The fit was done by maximising the likelihood:

$$\mathcal{L} = \sum_i^{mass} \sum_j^{tr(\mathcal{P}_{ev})} \sum_k^{X_E} \ln \left(\frac{\lambda_{i,j,k}^{N_{i,j,k}^{dat}}}{e^{\lambda_{i,j,k}} \cdot N_{i,j,k}^{dat}!} \right) . \tag{11}$$

To illustrate the fit results, the charm hadron X_E and $tr(\mathcal{P}_{ev})$ distributions for the different decay modes are shown in figures 3 to 6. The rates of charm hadrons in simulated $c\bar{c}$ and $b\bar{b}$ events were scaled according to the fitted rates of equation 10. The combinatorial background was subtracted from the data using a fit (similar to the one for the $N_{i,j,k}^{back}$) of the Monte Carlo background to the sidebands of the mass spectra obtained for each bin of X_E or $tr(\mathcal{P}_{ev})$.

6   Systematic uncertainties

Three major systematic error sources were considered in this analysis. The uncertainty in the Monte Carlo modelling of heavy quark production and decay could lead to changes in the predicted spectra of charm hadrons in $c\bar{c}$ and $b\bar{b}$ events. Problems in the simulation of the detector response effected the efficiency to identify charm hadron events. The fit method itself was also a potential source of systematic errors. The breakdown of the

Source	D^0	D^+	$D_s^+(\phi)$	$D_s^+(K^*)$	Λ_c^+	D^{*+}
$\tau(B^+) = 1.65 \pm 0.04$ ps	∓0.3	∓0.2	∓0.3	∓0.5	∓0.2	∓0.8
$\tau(B^0) = 1.56 \pm 0.04$ ps	∓0.3	∓0.3	∓0.4	∓0.3	∓0.3	∓0.8
$\tau(B_s^0) = 1.54 \pm 0.07$ ps	∓0.1	∓0.1	∓0.1	∓0.1	∓0.1	∓0.6
$\tau(\Lambda_b) = 1.24 \pm 0.08$ ps	∓0.0	∓0.2	∓0.0	∓0.0	∓0.3	∓0.9
$\tau(D^+) = 1.057 \pm 0.015$ ps	±0.0	±0.7	±0.1	±0.0	±0.1	±0.2
$\tau(D^0) = 0.415 \pm 0.004$ ps	±0.7	±0.1	±0.1	±0.1	±0.1	±0.2
$\tau(D_s^+) = 0.467 \pm 0.017$ ps	±0.0	±0.0	±0.6	±1.6	±0.1	±0.3
$\tau(\Lambda_c) = 0.206 \pm 0.012$ ps	±0.0	±0.0	±0.1	±0.2	±1.5	±0.3
$\langle X_E^c(D^*)\rangle = 0.510 \pm0.009$	±2.7	±1.5	±1.6	±1.7	±1.2	±1.1
$\langle X_E^b(B)\rangle = 0.702 \pm0.008$	±0.2	±0.3	±0.2	±0.3	±0.1	±0.3
$\epsilon_{b\to D} = 0.42 \pm0.07$	∓0.6	∓0.7	∓0.5	∓0.6	∓0.3	∓0.8
$n_{g\to c\bar{c}} = (2.38 \pm0.48)\%$	∓0.4	∓0.3	∓0.4	∓0.5	∓0.3	∓0.4
$P_{c\to D^+} = 0.221 \pm 0.020$	±0.2	±0.2	±0.3	±0.2	±0.1	±0.2
$P_{c\to D_s^+} = 0.112 \pm 0.027$	∓0.1	∓0.1	∓0.8	∓1.8	∓0.1	∓0.1
$P_{c\to c_{baryon}} = 0.084 \pm 0.022$	∓0.1	∓0.0	∓0.2	∓0.0	∓0.3	∓0.4
RICH + dE/dx	±0.4	±1.5	±0.9	±2.5	±2.3	-
VD-hits	±0.6	±0.8	±0.8	±0.9	±0.9	-
$\mathcal{P}(\chi^2)$ vertex fit	-	±1.0	±1.0	±1.2	±1.1	-
$L\,vs.\,X_E$	±2.1	±1.7	±1.2	±2.1	±1.7	-
Tracking	±0.6	±0.9	±0.9	±0.9	±0.9	±0.9
b tagging	±0.7	±0.5	±0.6	±3.7	±5.5	±2.2
MC statistics	±1.7	±2.1	±3.8	±7.8	±6.1	±1.6
$m(D,\Lambda)$ mean	±0.3	±0.2	±0.4	±1.4	±1.4	±0.3
$m(D,\Lambda)$ width	±0.1	±0.1	±0.3	±3.9	±1.5	±0.5
Reflections	∓0.1	∓0.7	∓0.6	∓4.8	∓0.8	∓0.4
Total	±4.1	±4.0	±4.8	±11.7	±10.4	±3.6

Table 6: *Systematic error in % on $R_c P_{c\to D,\Lambda}BR$.*

relative systematic errors on the measurements of $R_c P_{c\to D,\Lambda}BR$ and $R_b P_{b\to D,\Lambda}BR$ are given in tables 6 and 7, respectively.

The Monte Carlo modelling of heavy flavour production and decay affected the fit result in different ways. A change of the parameters led to a different shape of the Monte Carlo signal spectra. Furthermore the selection efficiency and b tagging depended on the heavy flavour production and decay properties. Therefore it was necessary to correct for inadequate simulation settings. The corrections were done using the JETSET program to produce the required distribution and compare it to the full simulation before detector acceptance. The normalized ratio of the two spectra was used as a weight to modify the Monte Carlo shape in equation 10. To estimate the systematic error, the input value was changed within its quoted error and the procedure was repeated.

The simulated b lifetimes were corrected separately for B^+, B^0, B_s^0 and Λ_b, using their world average values [17]. For the systematic uncertainties, all the b lifetime distributions were regenerated at $\pm1\sigma$ and the fit was performed again. The charm hadron lifetimes were also corrected separately for D^+, D^0, D_s^+ and Λ_c [17].

Source	D^0	D^+	$D_s^+(\phi)$	$D_s^+(K^*)$	Λ_c^+	D^{*+}
$\tau(B^+) = 1.65 \pm 0.04$ ps	± 0.7	± 0.5	± 0.6	± 0.9	± 0.7	± 0.5
$\tau(B^0) = 1.56 \pm 0.04$ ps	± 1.0	± 1.2	± 1.1	± 0.7	± 0.9	± 1.1
$\tau(B_s^0) = 1.54 \pm 0.07$ ps	± 0.3	± 0.2	± 0.9	± 1.0	± 0.1	± 0.4
$\tau(\Lambda_b) = 1.24 \pm 0.08$ ps	± 0.6	± 0.6	± 0.6	± 0.8	± 3.4	± 0.6
$\tau(D^+) = 1.057 \pm 0.015$ ps	± 0.1	± 0.2	± 0.0	± 0.0	± 0.1	± 0.2
$\tau(D^0) = 0.415 \pm 0.004$ ps	± 0.2	± 0.1	± 0.0	± 0.0	± 0.1	± 0.2
$\tau(D_s^+) = 0.467 \pm 0.017$ ps	± 0.1	± 0.1	± 0.0	± 0.0	± 0.1	± 0.2
$\tau(\Lambda_c) = 0.206 \pm 0.012$ ps	± 0.0	± 0.1	± 0.0	± 0.1	± 0.1	± 0.3
$\langle X_E^c(D^*)\rangle = 0.510 \pm 0.009$	∓ 1.1	∓ 1.1	∓ 0.3	∓ 0.6	∓ 1.2	∓ 0.3
$\langle X_E^b(B)\rangle = 0.702 \pm 0.008$	± 3.1	± 1.8	± 1.9	± 2.3	± 2.9	± 1.1
$\epsilon_{b\to D} = 0.42 \pm 0.07$	∓ 3.8	∓ 1.2	∓ 1.8	∓ 2.2	∓ 0.8	∓ 1.8
$n_{g\to c\bar c} = (2.38 \pm 0.48)\%$	∓ 0.3	∓ 0.2	∓ 0.2	∓ 0.2	∓ 0.3	∓ 0.3
$P_{c\to D^+} = 0.221 \pm 0.020$	∓ 0.3	∓ 0.3	∓ 0.2	∓ 0.2	∓ 0.3	∓ 0.2
$P_{c\to D_s^+} = 0.112 \pm 0.027$	± 0.1	± 0.1	± 0.2	± 0.3	± 0.1	± 0.1
$P_{c\to c_{baryon}} = 0.084 \pm 0.022$	± 0.3	± 0.2	± 0.2	± 0.3	± 0.1	± 0.2
RICH + dE/dx	± 0.4	± 1.5	± 0.9	± 2.5	± 2.3	-
VD-hits	± 0.6	± 0.8	± 0.8	± 0.9	± 0.9	-
$\mathcal{P}(\chi^2)$ vertex fit	-	± 1.0	± 1.0	± 1.2	± 1.1	-
$L\,vs.\,X_E$	± 2.1	± 1.7	± 1.2	± 2.1	± 1.7	-
Tracking	± 0.6	± 0.9	± 0.9	± 0.9	± 0.9	± 0.9
b tagging	± 0.8	± 1.3	± 0.8	± 3.4	± 2.1	± 2.5
MC statistics	± 2.0	± 2.7	± 2.9	± 4.7	± 5.5	± 1.4
$m(D,\Lambda)$ mean	± 0.1	± 0.1	± 0.8	± 1.9	± 1.6	± 0.2
$m(D,\Lambda)$ width	± 0.1	± 0.2	± 0.5	± 2.6	± 1.1	± 0.4
Reflections	∓ 0.1	∓ 0.5	∓ 0.5	∓ 2.0	∓ 0.9	∓ 0.6
Total	± 6.1	± 5.0	± 5.0	± 8.7	± 8.6	± 4.0

Table 7: *Systematic error in % on $R_b P_{b\to D,\Lambda} BR$.*

A similar procedure allowed for the uncertainty of the mean $\langle X_E^c(D)\rangle$ and $\langle X_E^b(B)\rangle$. JETSET was used to generate the $\langle X_E\rangle$ distributions of all charm ground states according to $\langle X_E^c(D^*)\rangle = 0.510 \pm 0.005 \pm 0.008$, $\langle X_E^b(B)\rangle = 0.702 \pm 0.008$ [11]. The second error on $\langle X_E^c(D^*)\rangle$ is due to the choice of the fragmentation function as proposed in [11]. It has been shown in [11,12], that the Collins and Spiller (or the Kartvelishvili) parametrisation produce similar results slightly higher/lower than the Peterson one. Therefore the Peterson parametrisation was taken to define the average and the error on $\langle X_E^c(D^*)\rangle$ was increased to reflect the uncertainty in the fragmentation function. The energy spectrum of D mesons in the B rest frame had been measured by CLEO [18]. This $\langle X_E^b(D)\rangle$ spectrum included the contributions from $B \to D\,X$ and $B \to D\bar{D}\,X$. It could be parameterised in terms of a Peterson function with a coefficient $\epsilon_{b\to D} = 0.42 \pm 0.07$ [11].

The corrections were applied on all simulated charm hadron states separately for $b\bar{b}$ and $c\bar{c}$ events. The resulting X_E distribution of the sum of all charm hadron ground states in $c\bar{c}$ events was found to be in agreement with the corresponding average of $\langle X_E^c(D^0, D^+)\rangle = 0.484 \pm 0.008$ [11]. The systematic uncertainties were calculated separately for $\langle X_E^c(D)\rangle$, $\langle X_E^b(B)\rangle$ and $\epsilon_{b\to D}$.

To account for gluon splitting into $c\bar{c}$ quark pairs, the $g \to c\bar{c}$ component was subtracted from the measured charm hadron spectra. Here the Monte Carlo prediction was scaled to reproduce the average multiplicity $n_{g \to c\bar{c}} = (2.38 \pm 0.48)\%$ [19]. The systematic uncertainty was obtained by varying this value within its error.

The separation between $b\bar{b}$ and $c\bar{c}$ events obtained from the impact parameter tag depended on the rate of D^+ and D^0 meson production in $c\bar{c}$ events. Therefore the rates of charm hadrons in the hemisphere opposite to the reconstructed D or Λ were fixed to the present averages $P_{c \to D^+} = 0.221 \pm 0.020$, $P_{c \to D_s^+} = 0.112 \pm 0.027$ and $P_{c \to c_{baryon}} = 0.084 \pm 0.022$ [26]. The D^0 rate was calculated from these values according to:

$$P_{c \to D^0} = 1 - P_{c \to D^+} - P_{c \to D_s^+} - P_{c \to c_{baryon}} . \tag{12}$$

A 1σ error variation on each fraction was included in the systematic error, leaving the D^0 fraction free to keep the sum constant.

However these rates will be free parameters in the final calculation of R_c presented in section 8.2, where the ingoing measurements are merged with a χ^2 minimisation to obtain the best set of results with respect to their correlated errors.

A good description of the detector acceptance was needed to extract the efficiency correction from the simulation. Therefore a careful tuning to correct for residual problems in the Monte Carlo description was done in all stages of the analysis. The decay channel $D^{*+} \to (K^-\pi^+)\pi^+$ was chosen to study the systematic errors due to the selection of charm hadrons. It was analysed in a window around the mass difference between the D^0 and the remaining slow π^+, resulting in very pure samples for data and simulation. Since this decay channel was also used in the analysis, none of the cuts discussed in the following have been performed on it.

To test the effect of a cut used to reconstruct a given decay channel, it is applied to the D^{*+} samples. The inefficiencies $\bar{\epsilon}$ were computed in data from a fit to the D^{*+} mass spectrum of rejected events and compared to the Monte Carlo result. For a residual discrepancy between these inefficiencies, a factor:

$$f_{corr} = \frac{1 - \bar{\epsilon}_{data}}{1 - \bar{\epsilon}_{MC}} \tag{13}$$

was introduced to correct the Monte Carlo description of the efficiency for the given decay channel. The relative statistical uncertainty on the correction factor was taken as a systematic error.

The combined RICH and dE/dx identification used to select the different charm hadrons was tested using the kaon from the D^0 in the D^{*+} channel. For each decay mode the same cuts were applied to the D^{*+} sample. To reconstruct the $D_s^+(\bar{K}^*)$ channel, both kaons were required to be tagged. Here the correction applied is the product of two correction factors, one for the π veto on the K^- from $\bar{K}^*$ and one for the tag on the K^+. For the $D_s^+(\phi)$ channel only one kaon had to be identified. A very pure $\Lambda^0 \to p\pi^-$ sample was used to test the proton identification on the Λ_c^+ channel. Only protons from Λ^0 with a momentum above the cut applied to the Λ_c^+ sample were used for this study.

The requirement of all candidate tracks to have at least one VD hit associated was tested for the three body decays with the $D^{*+} \to D^0\pi^+$ decay tracks. In case of the D^0, the slow pion was not required to have any VD hits.

The cut on the vertex fit χ^2 probability $\mathcal{P}(\chi^2)$ was also tested using the D^{*+} sample. Fitting all three decay products of the $D^{*+} \to (K^-\pi^+)\pi^+$ into one common vertex is a good approximation for a three body decay vertex, since the pion from the D^{*+} decay has a small transverse momentum relative to the D^0 direction. This is a test that, in the

situation of three close tracks issued from a charm hadron decay, the vertex reconstruction is made the same way in data and simulation. The average correction of about 4.5% reflects the incomplete modeling of the vertex reconstruction in the simulation.

The energy-dependent cuts on the measured decay length L of the charm hadron was also tested using the D^0 from the D^{*+} sample. The correction for the D^+ channel was computed by scaling the measured D^0 decay length by the lifetime ratio $\tau(D^+)/\tau(D^0)$.

A summary of all correction factors applied to the fitted rates can be found in table 8. It has been checked that the product of the efficiency correction factors obtained was in good agreement with the overall correction for the RICH + dE/dx, VD hits, $\mathcal{P}(\chi^2)$ and L cuts.

The charged track reconstruction efficiency was another possible source of systematic errors. In reference [20] the tracking efficiency in DELPHI has been estimated to be $(98.9 \pm 0.1)\%$. The difference between data and simulation in the region of the TPC ϕ boundaries was estimated to be $\pm 0.2\%$. Taking $\pm 25\%$ of the average inefficiency as a systematic error and adding the boundary effect leads to an error on the reconstruction of $\pm 0.3\%$ per track. This error enters in the systematic error table to the power of the multiplicity for a given decay mode, assuming 100 % correlation between all years of data taking and all channels. An additional crosscheck was done in reference [20] on the efficiency for tracks beeing reconstructed using the VD. It was found that the efficiency corrected multiplicity of tracks in the VD agrees better than 0.3 % with the average Z^0 multiplicity [17].

The effect due to the efficiency of the b tagging was studied in reference [21] using a tuning determined independently on data and simulation. A residual difference in the b efficiency of 3% per jet between data and simulation was found. The corrections to the physics parameters in the simulation generator mentioned above accounted for this difference.

Furthermore, the effect due to the resolution of the b tagging has been estimated by exchanging the b tag tunings of data and simulation.

Particle	RICH($+dE/dx$)	$L\,vs.\,X_E$	$\mathcal{P}(\chi^2)$	VD-hits
D^0	0.9989±0.0042	1.0048±0.0206	–	1.0067±0.0064
D^+	0.9528±0.0148	1.0137±0.0175	0.9579±0.0097	1.0017±0.0084
$D_s^+(\phi)$	1.0054±0.0093	1.0113±0.0117	0.9563±0.0099	1.0017±0.0084
$D_s^+(K^*)$	0.9875±0.0250	1.0109±0.0206	0.9519±0.0122	1.0110±0.0088
Λ_c^+	0.9339±0.0226	1.0096±0.0174	0.9501±0.0114	1.0110±0.0088

Table 8: *Correction factors applied to the selection efficiencies of the simulation.*

The uncertainty due to the statistical error of the simulated sample is given in tables 6 and 7. For the D^0, D^+ and D^{*+} this error was included directly in the χ^2 definition. For the binned likelihood fit to the D_s^+ and Λ_c^+ spectra, the error due to the limited number of simulated events was evaluated using a statistical method. The distribution of 3000 fit results using random Monte Carlo sets reflected the total statistical error while the error obtained from the fits only included the statistical error of the data set itself. Hence the width of the distribution was taken as the contribution from the Monte Carlo statistics.

The shape of the mass signal was also a possible source of systematics. The variation of its mean and width was included in the systematic errors shown in the tables.

The rate of reflections affected the background shape under the signal. Changes in the rate lead to variations in the fit result, especially for the $D_s^+(\bar{K}^*)$ channel. The systematic error assigned corresponded to a 30% variation of the reflection rates.

Finally for the D^0, the effect of wrongly identifying a true π^- as a K^- has been studied by applying the D^0 kaon identification and helicity cuts to the D^{*+} sample. The ratio $K\pi/\pi K$ was estimated in data and simulation and a correction to the shape of the πK distribution in the simulation was applied. The systematic effect due to this source was found to be negligible.

All systematic uncertainties for the different decay channels were summed up quadratically to obtain the total systematic errors given in tables 6 and 7. In the following calculations of the combined D_s^+ rate, R_c and n_c, the systematics due to the Monte Carlo modelling and the detector acceptance were assumed to be fully correlated between the different channels.

7 Fit results

The products $R_c P_{c \to D, \Lambda_c} BR$ and $R_b P_{b \to D, \Lambda_c} BR$ were measured from a 3-dimensional fit to the charm hadron mass spectra, the scaled energy X_E and the impact parameter information $tr(\mathcal{P}_{ev})$. The results are shown in table 9, where BR denotes the branching ratio of each decay given in the first column. The first error denotes the statistical uncertainty, the second error corresponds to the systematic error discussed above. The numbers include the efficiency corrections given in table 8. The D_s^+ rates were corrected for the branching ratio $BR(\phi \to K^- K^+) = (49.1 \pm 0.8)\%$ [17] and $BR(\bar{K}^*(892) \to K^- \pi^+) = 2/3$. The correlation is given in the last column.

Mode	$R_c P_{c \to D, \Lambda_c} BR \times 10^3$	$R_b P_{b \to D, \Lambda_c} BR \times 10^3$	$correlation$ %
$D^0 \to K^- \pi^+$	$3.570 \pm 0.100 \pm 0.146$	$4.992 \pm 0.162 \pm 0.304$	-46
$D^+ \to K^- \pi^+ \pi^+$	$3.494 \pm 0.116 \pm 0.140$	$4.525 \pm 0.204 \pm 0.226$	-38
$D_s^+ \to \phi(1020)\pi^+$	$0.765 \pm 0.069 \pm 0.037$	$1.259 \pm 0.100 \pm 0.063$	-30
$D_s^+ \to K^*(892)K^+$	$0.624 \pm 0.122 \pm 0.073$	$1.179 \pm 0.159 \pm 0.102$	-30
$\Lambda_c^+ \to p K^- \pi^+$	$0.743 \pm 0.155 \pm 0.078$	$0.962 \pm 0.187 \pm 0.083$	-30
$D^{*+} \to (K^- \pi^+)\pi^+$	$1.089 \pm 0.027 \pm 0.039$	$1.315 \pm 0.035 \pm 0.053$	-34

Table 9: *Results on $R_{c(b)} P_{c(b) \to D, \Lambda_c} BR(D, \Lambda_c \to X)$ from the combined fit to the data. The first error is statistical, the second systematical.*

Based on these numbers, the product of $R_{c(b)}$ and the production probability $P_{c(b) \to D, \Lambda_c}$ can be calculated for the charm counting using the branching ratios given in table 10 according to reference [17].

No precise measurement for the branching ratio $D_s^+ \to \bar{K}^*(892)K^+$ has been made. Therefore the ratio $BR(D_s^+ \to \bar{K}^*(892)K^+)/BR(D_s^+ \to \phi(1020)\pi^+)$ was used. The results for both decay modes are compared in table 11. The third error given in addition to the statistical and systematic error corresponds to the uncertainty on the branching ratios. The average given in the table was computed taking all correlations into account. The variations on the $P_{c \to D, c_{baryon}}$ from section 6 could not be used here to calculate the average: They have been defined as further systematic uncertainties and reassigned in

Mode	branching fraction
$D^0 \to K^- \pi^+$	0.0385 ± 0.0009
$D^+ \to K^- \pi^+ \pi^+$	0.090 ± 0.006
$D_s^+ \to \phi(1020)\pi^+$	0.036 ± 0.009
$\frac{BR(D_s^+ \to \bar{K}^* K^+)}{BR(D_s^+ \to \phi \pi^+)}$	0.95 ± 0.10
$\Lambda_c^+ \to p K^- \pi^+$	0.050 ± 0.013

Table 10: *Branching fractions used for the charm fraction measurements [17].*

the calculation of R_c after the averaging. The statistical correlation of the averages for $c\bar{c}$ and $b\bar{b}$ events is -30%.

Mode	$R_c P_{c \to D_s^+} \times 10^2$	$R_b P_{b \to D_s^+} \times 10^2$
$D_s^+ \to \phi(1020)\pi^+$	$2.189 \pm 0.198 \pm 0.108 \pm 0.562$	$3.596 \pm 0.286 \pm 0.179 \pm 0.924$
$D_s^+ \to K^*(892)K^+$	$1.877 \pm 0.366 \pm 0.221 \pm 0.521$	$3.545 \pm 0.478 \pm 0.308 \pm 0.984$
average	$2.129 \pm 0.175 \pm 0.107 \pm 0.539$	$3.594 \pm 0.246 \pm 0.182 \pm 0.913$

Table 11: *Results on $R_{c(b)} P_{c(b) \to D_s^+}$ including correlations. The first error is statistical, the second systematic and the third is due to the error on the branching ratio.*

A summary of the measured rates of D^0, D^+, D_s^+ and Λ_c^+ from $c\bar{c}$ and $b\bar{b}$ events is given in table 12.

Mode	$R_c P_{c \to D, \Lambda_c} \times 10^2$	$R_b P_{b \to D, \Lambda_c} \times 10^2$
D^0	$9.274 \pm 0.260 \pm 0.380 \pm 0.217$	$12.967 \pm 0.423 \pm 0.790 \pm 0.310$
D^+	$3.839 \pm 0.128 \pm 0.152 \pm 0.253$	$4.973 \pm 0.224 \pm 0.191 \pm 0.317$
D_s^+	$2.129 \pm 0.175 \pm 0.107 \pm 0.539$	$3.594 \pm 0.246 \pm 0.182 \pm 0.913$
Λ_c^+	$1.487 \pm 0.311 \pm 0.157 \pm 0.387$	$1.924 \pm 0.374 \pm 0.166 \pm 0.504$

Table 12: *Contributions to charm counting in $c\bar{c}$ and $b\bar{b}$ events. The first error is statistical, the second systematic and the third is due to the error on the branching ratio.*

8 Measurements of R_c

Two methods were used to extract R_c from the fit results. The first relied on the D^{*+} production rate from charm events and the probability for c quarks to give a D^{*+} as measured by DELPHI. The second used the charm counting in $c\bar{c}$ events.

8.1 R_c from the D^{*+} production rate

R_c can be obtained from the ratio of the production rate $R_c P_{c \to D^{*+}} BR(D^{*+} \to (K^- \pi^+)\pi^+)$ given in table 9 and the fragmentation probability $P_{c \to D^{*+}} BR(D^{*+} \to D^0 \pi^+)$.

Using $BR(D^0 \to K^-\pi^+) = 0.0385 \pm 0.0009$ [17] the following rate is obtained:

$$R_c P_{c\to D^{*+}} BR(D^{*+} \to D^0\pi^+) = 0.02829 \pm 0.00070(stat) \pm 0.00102(syst) \pm 0.00066(Br) . \quad (14)$$

DELPHI has measured $P_{c\to D^{*+}} BR(D^{*+} \to D^0\pi^+) = 0.174 \pm 0.010 \pm 0.004$ [5] using a double tag method based on the detection of exclusively reconstructed D mesons accompanied in the opposite hemisphere by D^{*+} decays, which were inclusively reconstructed from the p_T^2 spectra of slow pions with respect to the jet-axis.

The main contributions to the common systematics with the $R_c P_{c\to D^{*+}} BR(D^{*+} \to D^0\pi^+)$ measurement are due to the variation of the $\langle X_E^c(D^*)\rangle$, $\langle X_E^b(B)\rangle$ and $\epsilon_{b\to D}$ values. The influence due to the ratio $r = R_b P_{b\to D^{*+}}/R_c P_{c\to D^{*+}}$ with $D = D^{*+}, D^+, D^0$ is found to be small. An important systematic effect is due to the dependence between $P_{c\to D^{*+}}$ and R_c itself. The rest of the systematics in the $P_{c\to D^{*+}}$ measurement is uncorrelated to the $R_c P_{c\to D^{*+}}$ measurement.

R_c is determined (using the measured D^{*+} rates from table 9, $P_{c\to D^{*+}} BR(D^{*+} \to D^0\pi^+)$ from above and the $BR(D^0 \to K^-\pi^+)$ from table 10) to be:

$$R_c = 0.1610 \pm 0.0104(stat) \pm 0.0077(syst) \pm 0.0043(BR) , \quad (15)$$

taking the correlations between the measurements into account.

8.2 R_c from the charm counting

For this measurement, R_c was given by the sum of all weakly decaying charm hadron rates. The results presented in table 12 only include Λ_c^+ production. The rates for other weakly decaying strange charmed baryons were estimated from the light quark sector as in references [2] and [11]. The ratio Ξ^-/Λ was measured to be $(6.9 \pm 0.4)\%$ and the Ω^-/Λ ratio was $(0.44 \pm 0.08)\%$ [17]. Assuming equal production of Ξ^- and Ξ^0, about $14 \pm 5\%$ of strange charm baryon production is expected relative to the Λ_c rate. Therefore a contribution of 0.00208 ± 0.00074 for Ξ_c and Ω_c was added to the measured rates. Taking correlated systematics into account, R_c is obtained:

$$R_c = 0.1692 \pm 0.0047(stat) \pm 0.0063(syst) \pm 0.0074(BR) . \quad (16)$$

The DELPHI results for the full set of parameters as used by the LEP heavy flavour working group are given in table 13 together with the correlation matrix.

parameter	value	error	R_c	$P_{c\to D^+}$	$P_{c\to D_s^+}$	$P_{c\to c_{baryon}}$
R_c	0.1692	0.0109	1.00	-.31	0.34	0.42
$P_{c\to D^+}$	0.2270	0.0182	-.31	1.00	-.36	-.39
$P_{c\to D_s^+}$	0.1251	0.0297	0.34	-.36	1.00	-.23
$P_{c\to c_{baryon}}$	0.0999	0.0327	0.42	-.39	-.23	1.00

Table 13: *The DELPHI results for the full set of parameters as used by the LEP heavy flavour working group with correlation matrix.*

9 Charm counting in b decays

To extract from table 12 the number of charm quarks per b decay, all decays to charm states have to be summed. This includes charmonia $c\bar{c}$ states, which count twice, and strange charm baryons.

Mode	$P_{b \to X_c} \times 10^2$
J/ψ	$1.12 \pm 0.12(stat) \pm 0.10(sys)$
ψ'	$0.48 \pm 0.22(stat) \pm 0.10(sys)$
χ_{c1}	$1.4 \pm 0.6(stat)^{+0.4}_{-0.2}(sys)$

Table 14: *DELPHI published charmonia rates from b decays.*

The $b \to charmonia$ rates given in table 14 have been measured by DELPHI [22]. From these numbers, the total rate of charmonia production in b decays can be estimated assuming a production ratio of $\eta_c : J/\psi : \chi_{c1} : \psi' = 0.57 : 1. : 0.27 : 0.31$ [23] for the different states. The J/ψ and χ_{c1} production rate due to radiative charmonia decays were estimated using $BR(\psi' \to \chi_{c1}\gamma) = (8.7 \pm 0.8)\%$, $BR(\psi' \to J/\psi X) = (54.2 \pm 3.0)\%$ and $BR(\chi_{c1} \to J/\psi\gamma) = (27.3 \pm 1.6)\%$ [17]. The total rate $P_{b \to charmonia\,X} = 0.0200 \pm 0.0024 \pm 0.0060$ was obtained. The first error reflects the error of the measurements and of the branching ratios, the second error corresponds to a $\pm 30\%$ uncertainty assigned to the theoretical prediction of reference [23].

Mode	$P_{b \to X_c} \times 10^2$
D^0	$60.05 \pm 1.96 \pm 3.65 \pm 1.44$
D^+	$23.01 \pm 1.04 \pm 1.14 \pm 1.47$
D_s^+	$16.65 \pm 1.14 \pm 0.84 \pm 4.27$
Λ_c^+	$8.90 \pm 1.73 \pm 0.77 \pm 2.33$
$charmonia(*2)$	$4.00 \pm 0.48 \pm 1.20$
total measured	$112.59 \pm 3.08 \pm 3.99 \pm 5.42$

Table 15: *Contributions to charm counting in $b\bar{b}$ events. The first error is statistical, the second systematic and the third is due to the branching ratios.*

The rates $R_b P_{b \to D, \Lambda_c}$ given in table 12 were translated into $P_{b \to D, \Lambda_c}$ using the present average $R_b = 0.21626 \pm 0.00074$ [26]. The summary of the measured contributions to the charm counting in $b\bar{b}$ events is shown in table 15. Since their calculation is correlated to the charm counting, the charm fractions $P_{c \to D, \Lambda_c}$ used were the DELPHI measurements given in table 13 of section 8.2. The production rate $P_{b \to \Xi_c X}$ is not measured. It was estimated as in reference [24]. CLEO [25] has measured the rates $P_{\bar{B} \to \Xi_c^+} = 0.008 \pm 0.005$ and $P_{\bar{B} \to \Xi_c^0} = 0.012 \pm 0.009$. The world average values [17] for rates of b hadrons in Z events are $(39.7^{+1.8}_{-2.2})\%$ for B^0 and B^+, $(10.5^{+1.8}_{-1.7})\%$ for B_s^0 and $(10.1^{+3.9}_{-3.1})\%$ for b-baryons. A rate of 0.018 ± 0.010 Ξ_c baryons from B mesons is obtained. Using the JETSET simulation $P_{b_{baryon} \to \Xi_c X} = 0.22 \pm 0.11$ is estimated, which adds 0.022 ± 0.013 to the total Ξ_c rate. Adding the Ξ_c baryon contribution, 0.040 ± 0.016, to the measured rates in table 15, the charm quark multiplicity in b decays, n_c is obtained:

$$n_c = 1.166 \pm 0.031(stat) \pm 0.059(syst) \pm 0.054(BR). \qquad (17)$$

10 Discussion on $\frac{V}{V+P}$

Isospin conservation suggests equal production rates of charged $(c\bar{d})$ and neutral $(c\bar{u})$ D mesons in the fragmentation of charm quarks in $c\bar{c}$ events. A difference in the observed D^0 and D^+ rates could arise from the difference between the D^{*0} and the D^{*+} decay rates. The D^{*+} can decay into $D^0\pi^+$, $D^+\pi^0$ or $D^+\gamma$ while, due to kinematics, the D^{*0} can only decay into $D^0\pi^0$ or $D^0\gamma$ [17]. Therefore the observed rate of $D^{*+} \to D^0\pi^+$ could be responsible for the difference between the D^0 and D^+ production rates.

If $f_d(c)$ is defined as the probability for a charm quark to fragment into a primary charged D or D^* meson (assumed equal to $f_u(c)$, similarly defined for the fragmentation to a neutral D or D^* meson), then the probabilities for a charm quark to fragment into the observed D^{*+}, D^0 and D^+ mesons are expressed as:

$$P_{c\to D^{*+}}B_* = Y\,f_d(c) \tag{18}$$
$$P_{c\to D^0} = (1+Y)\,f_d(c) \tag{19}$$
$$P_{c\to D^+} = (1-Y)\,f_d(c) \tag{20}$$

where B_* denotes the branching ratio $BR(D^{*+} \to D^0\pi^+)$. Y denotes the production fraction of $D^{*+} \to D^0\pi^+$, which can be written as $Y = B_* \cdot \frac{V}{V+P}$, where $\frac{V}{V+P}$ is defined as the ratio of the vector meson rate to the total vector+pseudoscalar meson rate. As a cross-check of this formulation, using the results from table 9, the following ratio is obtained:

$$\frac{P_{c\to D^0} - P_{c\to D^+}}{2P_{c\to D^{*+}}B_*} = 0.963 \pm 0.051(stat) \pm 0.054(syst) \pm 0.051(BR)\,, \tag{21}$$

Hence in $c\bar{c}$ events the result is compatible with one, suggesting that the observed difference between D^0 and D^+ rates is due to the D^* decay properties, while in b events only a rough agreement is found:

$$\frac{P_{b\to D^0} - P_{b\to D^+}}{2P_{b\to D^{*+}}B_*} = 1.171 \pm 0.076(stat) \pm 0.081(syst) \pm 0.052(BR)\,. \tag{22}$$

This ratio could be higher than one because of differences between the decay rates of $B \to \bar{D}^0 + X$ and $B \to D^- + X$.

The Y value can be obtained for $c\bar{c}$ events from a fit to equation (18-20) using the results from tables 9 and 10. With $B_* = 0.683 \pm 0.014$ [17], this leads to:

$$\frac{V}{V+P} = 0.620 \pm 0.014(stat) \pm 0.014(syst) \pm 0.025(BR)\,. \tag{23}$$

This result is four sigma below the naive spin counting expectation of 0.75, suggesting a significant production of D^* and D mesons from decays of higher D mass states. These decays can lower the observed D^*/D production ratio.

11 Conclusions

The results on R_c and n_c presented in this paper are based on the DELPHI data taken from 1992 to 1995. Two R_c measurements have been described, based on the D^{*+} production rate and on the overall charm counting. Combining these two measurements gives

$$R_c = 0.1665 \pm 0.0051(stat) \pm 0.0061(syst) \pm 0.0054(BR)\,, \tag{24}$$

including a statistical correlation of 20% between the D^0 and D^{*+} sample. The result on R_c improves the precision compared to previous DELPHI published results [6].

Good agreement is found with other LEP results [2], [3], [4] and the Standard Model prediction $R_c = 0.1723 \pm 0.0001^3$.

In $c\bar{c}$ events, the ratio of the vector rate to the total vector+pseudoscalar rate was found to be 0.620 ± 0.032, suggesting a significant contribution of D^* and D mesons produced from heavier D states.

The charm quark multiplicity in b decays, n_c, is determined to be:

$$n_c = 1.166 \pm 0.031(stat) \pm 0.059(syst) \pm 0.054(BR) . \tag{25}$$

A comparison of this measurement (together with the DELPHI results on semileptonic b branching ratio $B_{SL} = (10.65 \pm 0.11 \pm 0.23^{-.27}_{+.43})\%$ [27]) with the theoretical expectation from reference [28] is shown in figure 7. The result on n_c also agrees well with a previous DELPHI result $n_c = 1.147 \pm 0.041$ [29] using an indirect method to extract the charmless and double charm contribution from the b tagging probability spectrum. The results on the individual production rates in $b\bar{b}$ events agree well with OPAL [2] and ALEPH [24]. However, the different assumptions for strange charm baryon production made in section 9 give rise to larger differences between the measurements and the result, $n_c = 1.10 \pm 0.05$, reported by CLEO [25].

Acknowledgements

---

[3]For $M_Z = 91.1876 \pm 0.0020$, $M_H = M_Z$, $m_t = 174 \pm 4 GeV$ and $\alpha_s = 0.1214 \pm 0.0031$

References

[1] G. Altarelli and S.Petrarca, Phys. Lett. **B 261** (1991) 303;
I. Bigi et al., Phys. Lett. **B 323** (1994) 408.

[2] G. Alexander et al., OPAL Collaboration, Z. Phys. **C 72** (1996) 1.

[3] ALEPH Collaboration, *Study of Charm production in Z decays*, EPS-HEP'97

[4] K. Ackerstaff et al., OPAL Collaboration, Eur. Phys. J. **C 1** (1998) 439;
R. Barate et al., ALEPH Collaboration, Eur. Phys. J. **C 1** (1998) 557.

[5] U. Gasparini et al., DELPHI Collaboration, *Determination of $P(c \rightarrow D^{*+})$ and $BR(c \rightarrow \ell)$ at LEP*, CERN-EP/Paper220/Draft1 , 1998.

[6] P. Abreu et al., Z. Phys. **C 59** (1993) 533;
erratum-ibid C65 (1995) 709
P. Abreu et al., Z. Phys C66 (1995) 323

[7] P.Abreu et al., DELPHI Collaboration, Nucl. Inst. and Meth. **A 378** (1996) 57.

[8] T. Sjöstrand, Comp. Phys. Comm. **39** (1986) 347 ;
T. Sjöstrand and M.Bengtsson, Comp. Phys. Comm. **43** (1987) 367.

[9] P. Abreu et al., DELPHI Collaboration, Zeit. Phys. **C 71** (1996) 11.

[10] C. Peterson, D. Schlatter, J. Schmitt and P. Zerwas, Phys. Rev. **D27** (1983) 105.

[11] The LEP Electroweak Working Group, *A consistent treatment of systematic Errors for LEP electroweak Heavy Flavour Analyses*, LEPHF/94-01, DELPHI 94-23 PHYS 357;
The LEP Electroweak Working Group, *Presentation of LEP Electroweak Heavy Flavour Results for the Summer 1996 Conferences*, LEPHF/96-01, DELPHI 96-67 PHYS 627, 1996;
The LEP Electroweak Working Group, *Presentation of LEP Electroweak Heavy Flavour Results for the Summer 1998 Conferences*, LEPHF/98-01, DELPHI 98-118 PHYS 789, 1998.

[12] LEP Collaboration, Nucl. Inst. Meth. **A378** (1996) 101.

[13] J.D. Bjoerken and S.J. Brodsky, Phys. Rev. **D 1** (1970) 1416.

[14] P. Abreu et al., The Eur. Phys. J. **C5** (1998) 585

[15] H.A. Bethe, Annalen der Physik 5 (1930) 201.

[16] G. Borisov and C. Mariotti, Nucl. Instr. & Meth. **A372** (1996) 181.

[17] C. Caso et al., Review of Particle Physics, The Eur. Phys. J. **C3** (1998) 1.

[18] D. Bortoletto et al., CLEO Collaboration, Phys. Rev. **D 45** (1992) 21.

[19] R. Akers et al., OPAL Collaboration, Phys. Lett. **B 353** (1995) 595.

[20] P. Abreu et al., DELPHI Collaboration, Phys. Lett. **B 425** (1998) 399.

[21] P. Abreu et al., DELPHI Collaboration, CERN EP-98-180

[22] P. Abreu et al., DELPHI Collaboration, Phys. Lett. **B 341** (1994) 109.

[23] J.H. Kühn, S. Nussinov and R. Rüdel, Z. Phys. **C 5** (1980) 117.

[24] D. Buskulic et al., ALEPH Collaboration, Phys. Lett. **B 388** (1996) 648.

[25] L. Gibbons et al., CLEO Collaboration, Phys. Rev. **D 56** (1997) 3783.

[26] The LEP Electroweak Working Group, *A Combination of Preliminary Electroweak Measurements and Constraints on the Standard Model*, CERN-PPE/97-154, 1997.

[27] M. Calvi et al., *Measurement of the semileptonic b branching ratios and $\bar{\chi}_b$ from inclusive leptons in Z decays*, DELPHI 98-122 CONF 183, Vancouver 1998.

[28] M. Neubert and C.T. Sachrajda, Nucl. Phys. **B 483** (1997) 339.

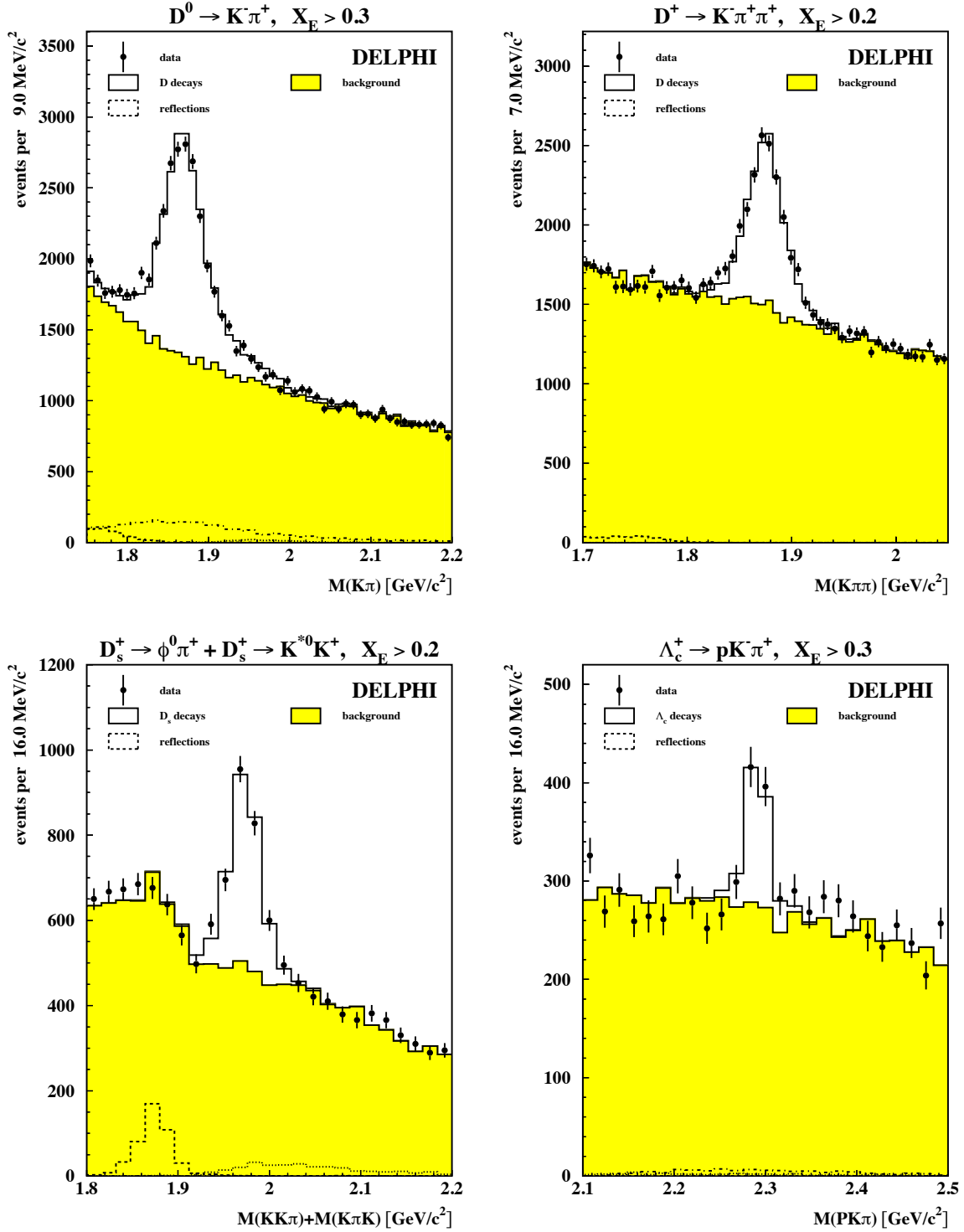[29] P. Abreu et al., DELPHI Collaboration, Phys. Lett. **B 426** (1998) 139.

Figure 1: *Invariant mass spectra of D^0, D^+, D_s^+ and Λ_c^+ in the given decay channels used for the charm counting. The dots are data and the histogram is simulation with the background shaded. Contributions from reflections are shown as a dotted line. The dot-dashed line in the D^0 spectrum shows $K\pi$ combinations, which are wrongly reconstructed as πK. The dashed peak in the D_s^+ spectrum shows the decay $D^+ \to K^- K^+ \pi^+$.*
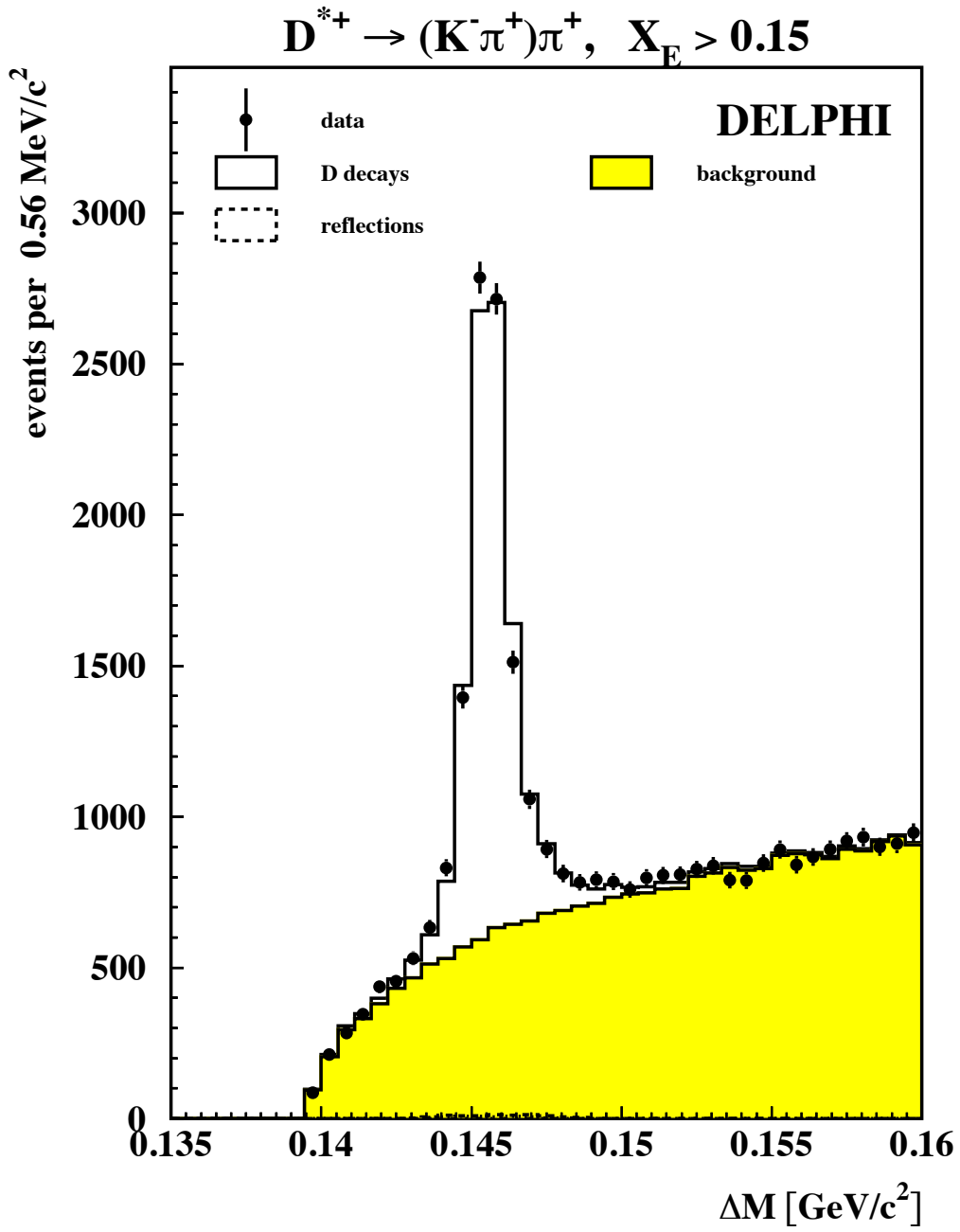
Figure 2: *Invariant mass difference $\Delta M = M(K^-\pi^+\pi^+) - M(K^-\pi^+)$ for the decay $D^{*+} \to D^0\pi^+$ followed by $D^0 \to K^-\pi^+$. The dots are data and the histogram is simulation with the background shaded.*
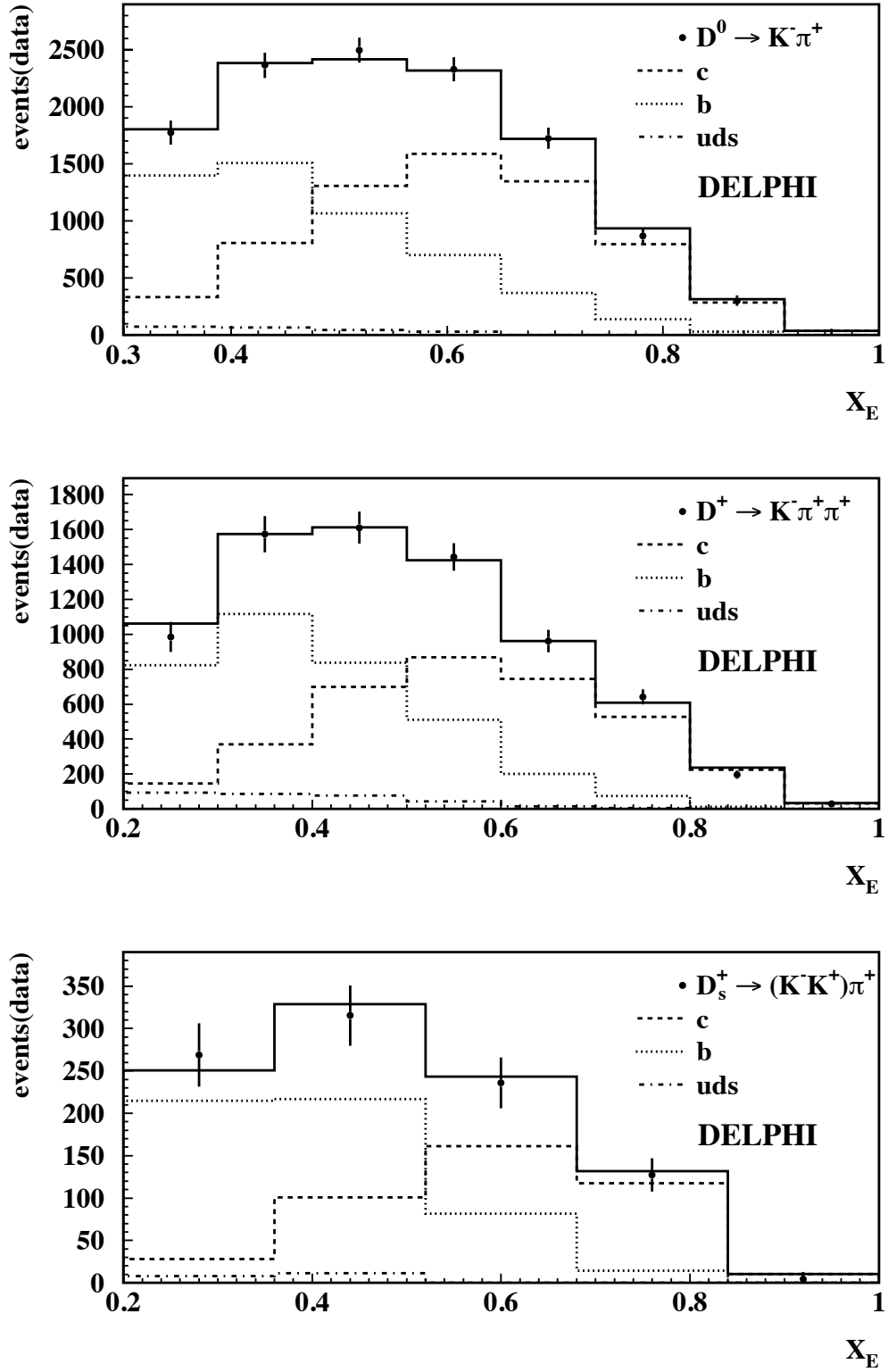
Figure 3: *Background subtracted X_E spectra for the decays $D^0 \rightarrow K^- \pi^+$ (top), $D^+ \rightarrow K^- \pi^+ \pi^+$ and $D_s^+ \rightarrow \phi(1020)\pi^+$ (bottom). No efficiency correction was applied. The reconstructed Monte Carlo spectra for $b\bar{b}$ and $c\bar{c}$ events were scaled in order to reproduce the fit results as described in the text.*
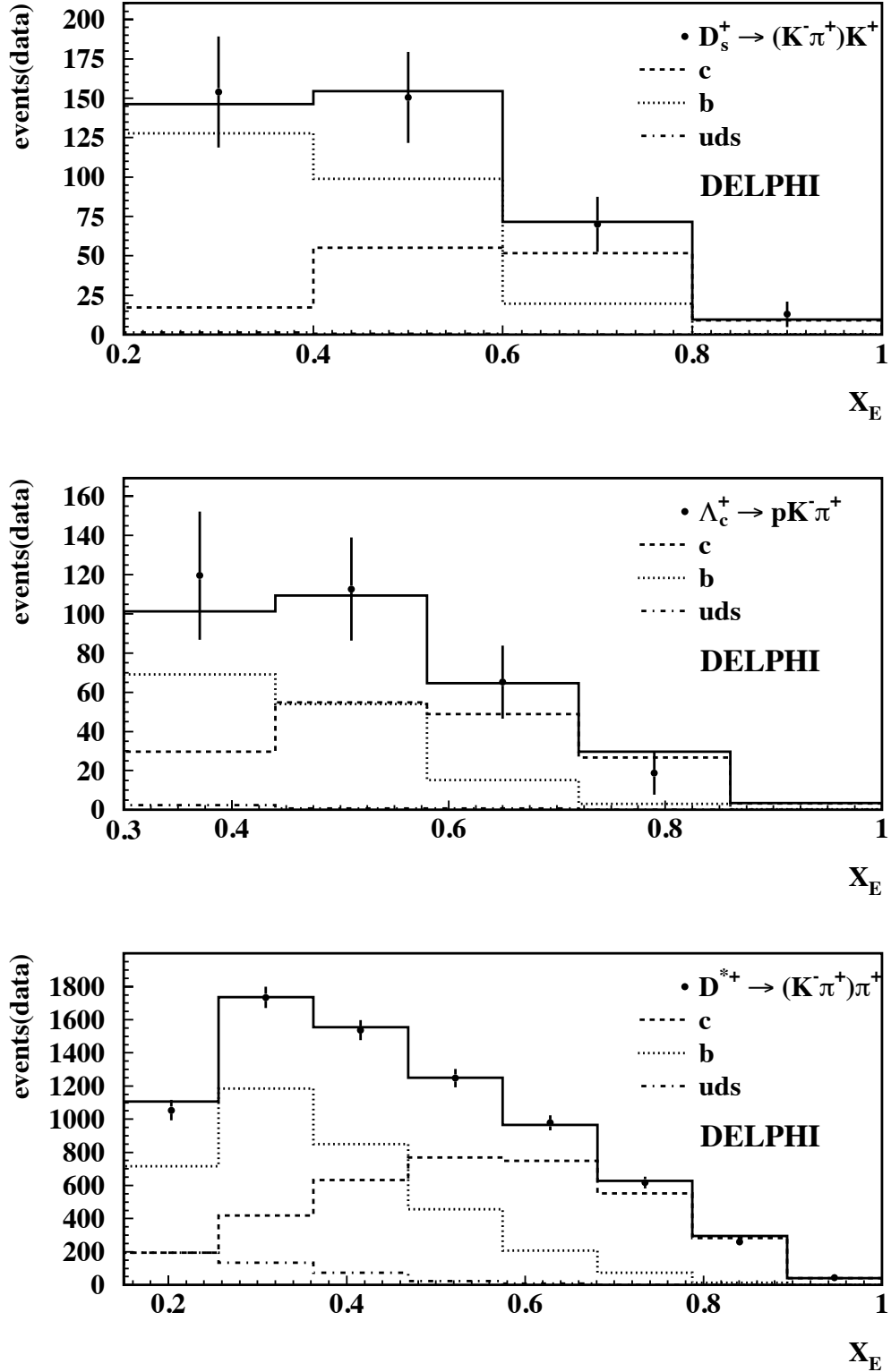
Figure 4: *Background subtracted X_E spectra for the decays $D_s^+ \rightarrow \bar{K}^*(892)K^+$ (top), $\Lambda_c^+ \rightarrow pK^-\pi^+$ and $D^{*+} \rightarrow D^0\pi^+$ followed by $D^0 \rightarrow K^-\pi^+$ (bottom). The same conditions as in the caption of figure 3 are valid.*
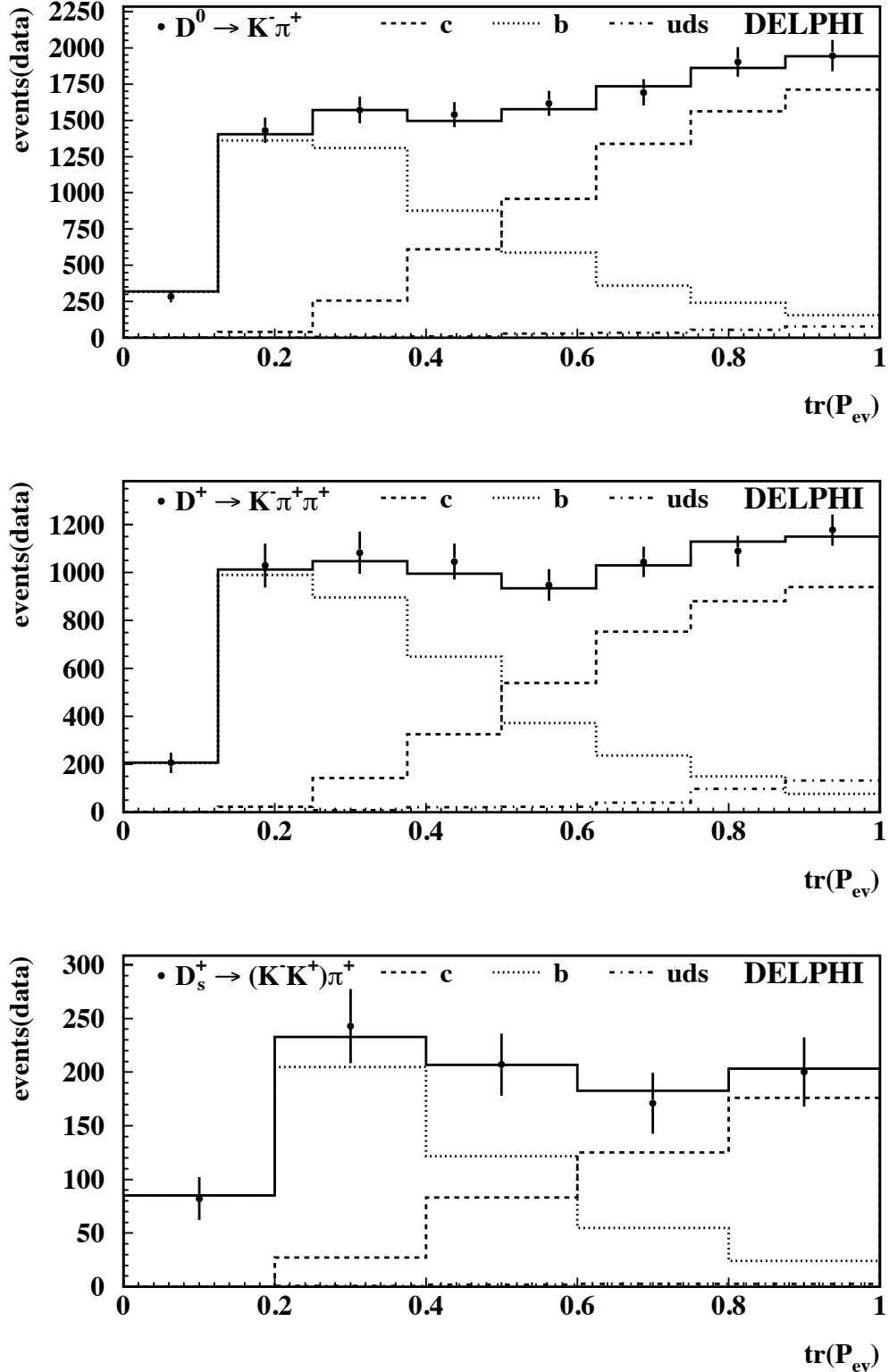
Figure 5: *Background subtracted* $tr(\mathcal{P}_{ev})$ *spectra for the decays* $D^0 \rightarrow K^-\pi^+$ *(top),* $D^+ \rightarrow K^-\pi^+\pi^+$ *and* $D_s^+ \rightarrow \phi(1020)\pi^+$ *(bottom). The same conditions as in the caption of figure 3 are valid.*
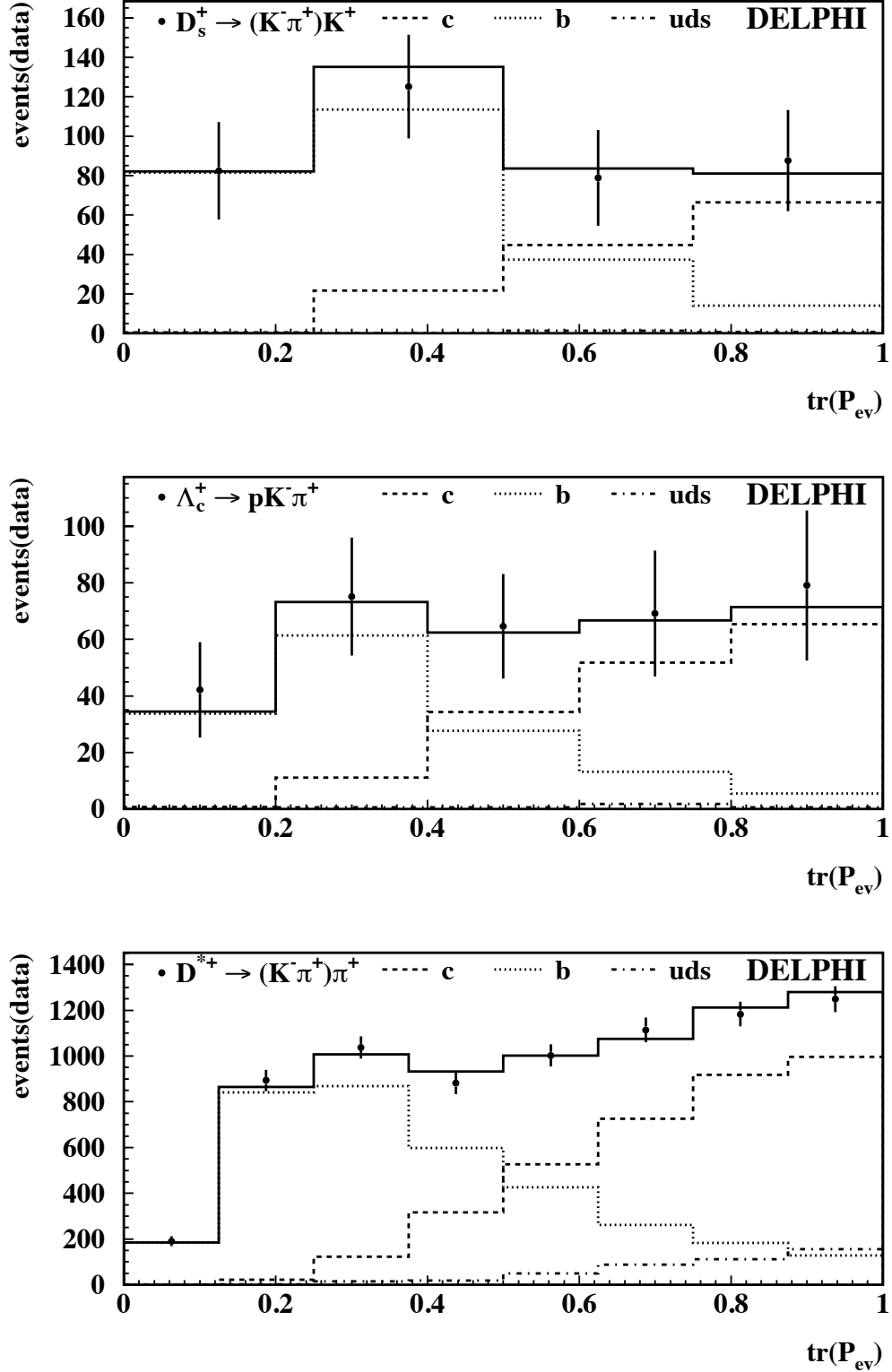
Figure 6: *Background subtracted $tr(\mathcal{P}_{ev})$ spectra for the decays $D_s^+ \to \bar{K}^*(892)K^+$ (top), $\Lambda_c^+ \to pK^-\pi^+$ and $D^{*+} \to D^0\pi^+$ followed by $D^0 \to K^-\pi^+$ (bottom). The same conditions as in the caption of figure 3 are valid.*
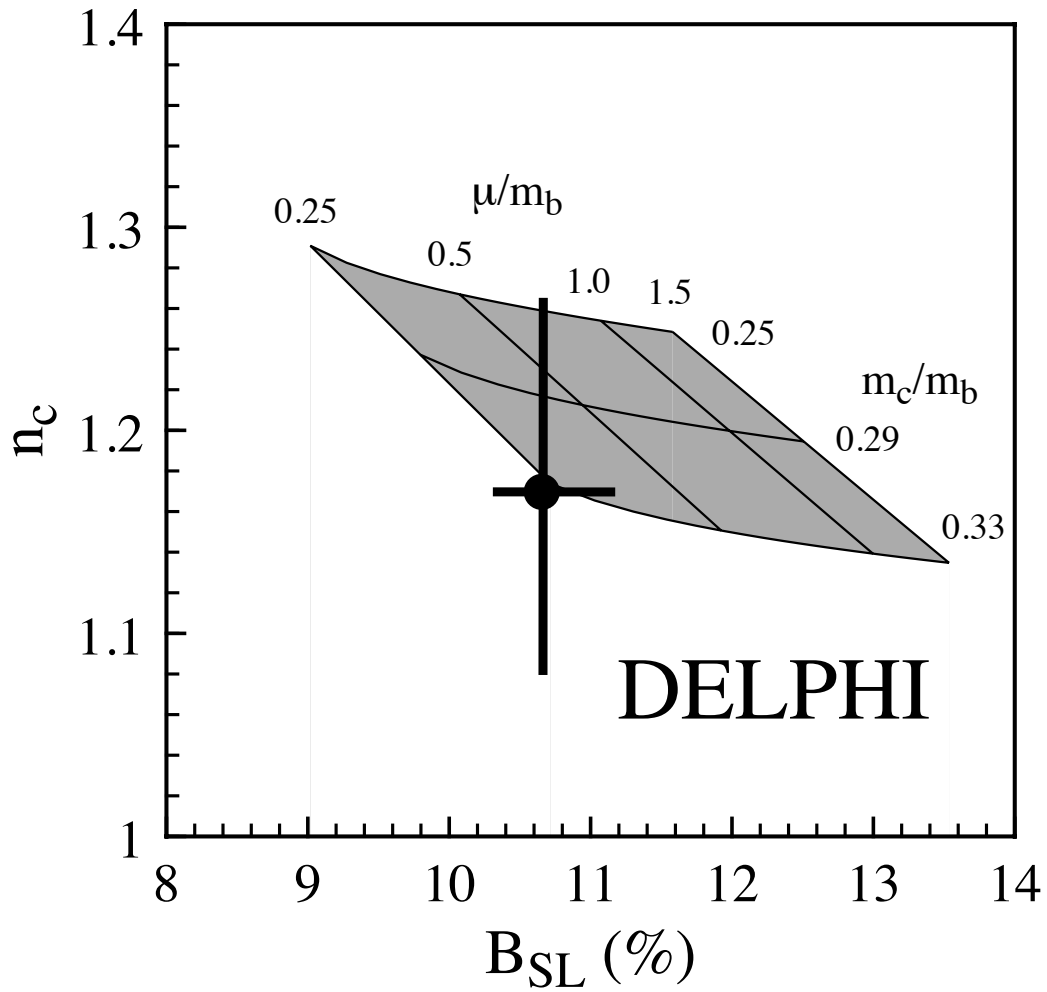
Figure 7: *Measured n_c and B_{SL} compared to the theoretical allowed region [28]. The shaded region is predicted by theory in the on-shell renormalisation scheme for different values of m_c/m_b and of the renormalisation scale μ/m_b.*